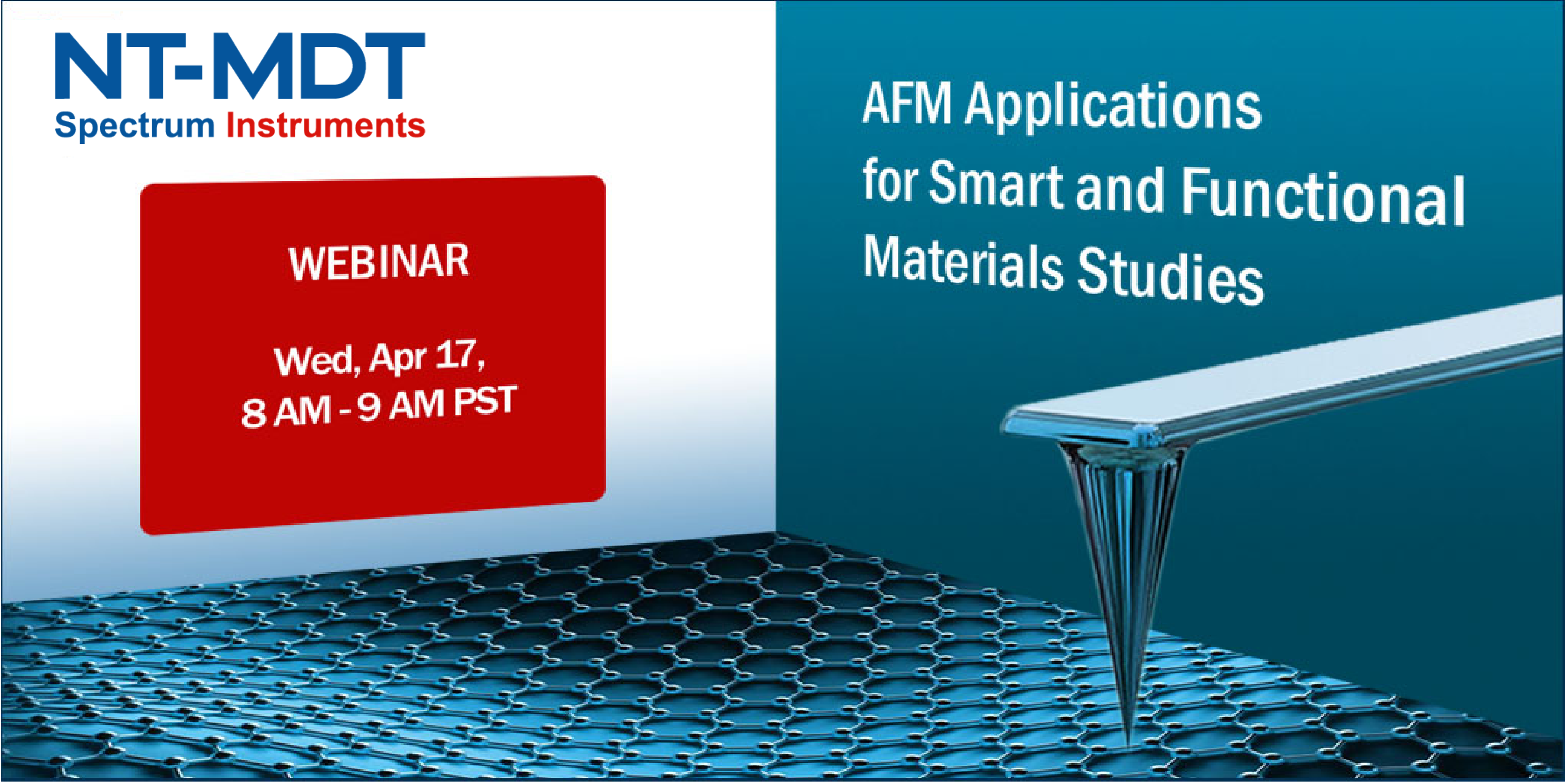

Stanislav I. Leesment, Ph.D

April 17th 2019

Skolkovo

Atomic Force (Scanning Probe) Microscope

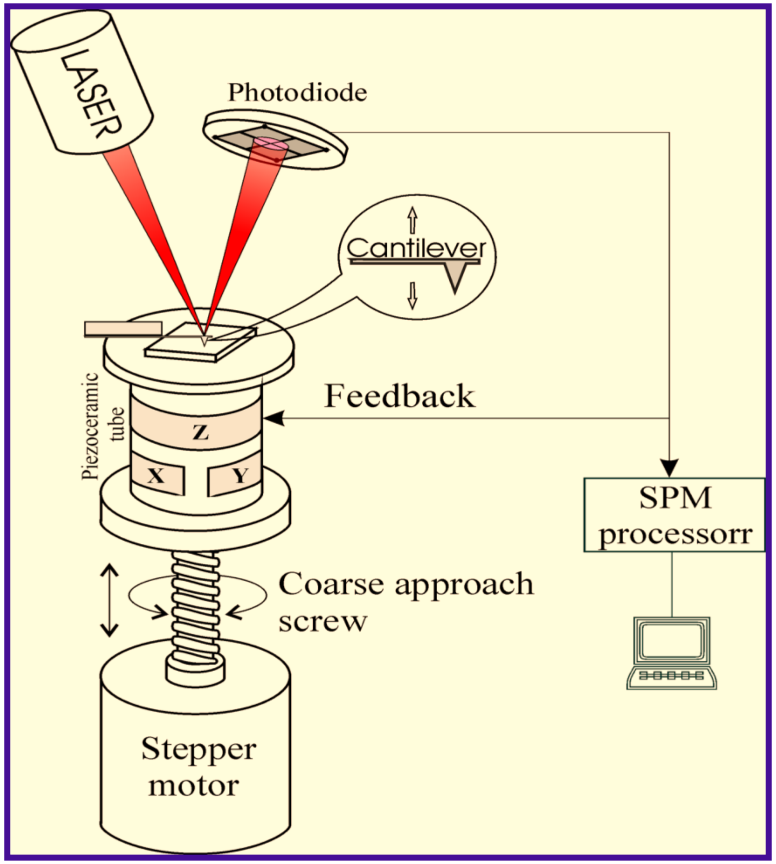

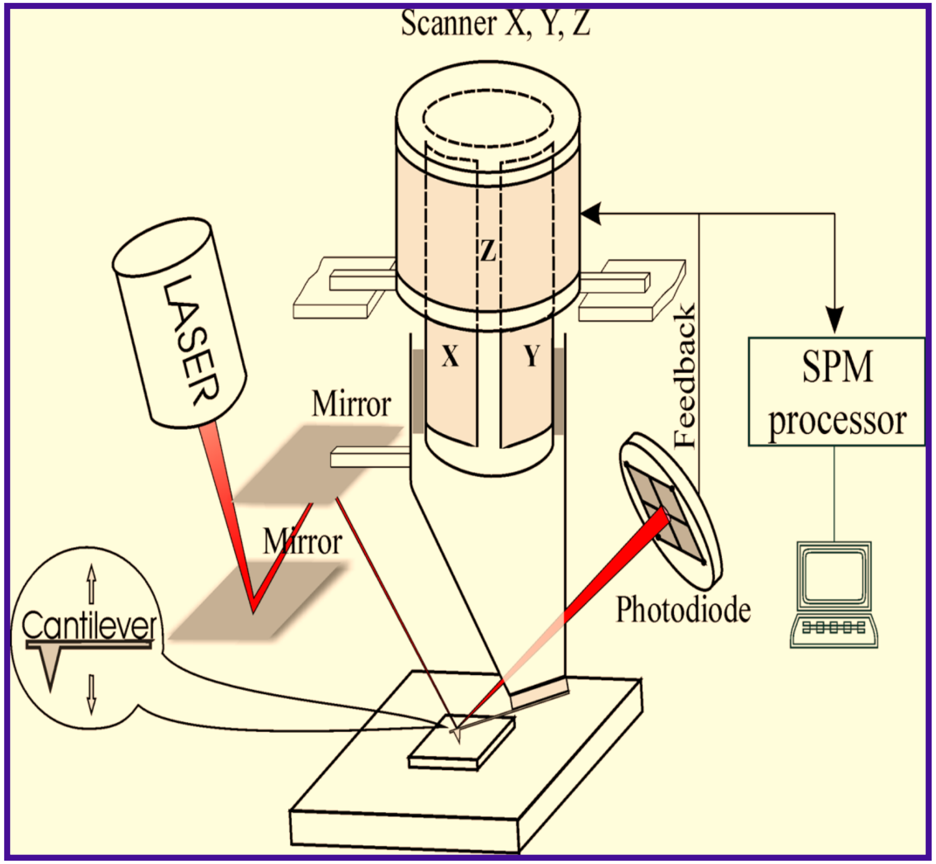

SAMPLE SCANNING

TIP SCANNING

AFM modes used for morphological studies

Contact Mode

Lateral force imaging, force modulation, contact resonance, PFM

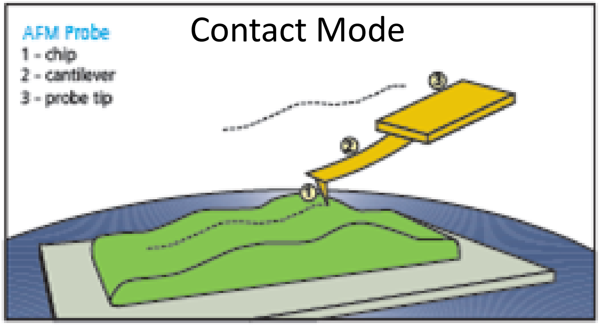

Oscillatory Resonant Modes

Amplitude modulation with phase and frequency imaging, frequency modulation, single- and double pass methods

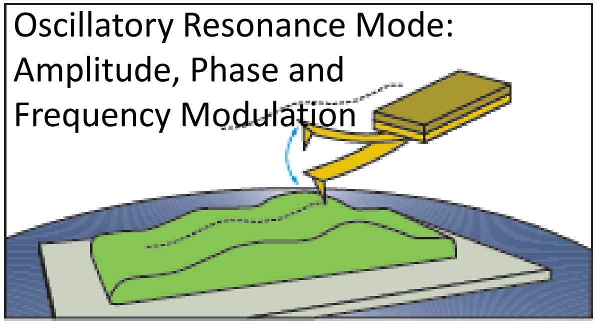

Oscillatory Non-Resonant Modes

Jumping mode, HybriD™ mode, etc

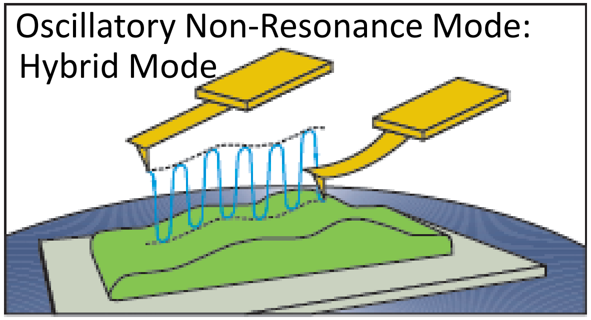

AM-AFM (Tapping) Mode

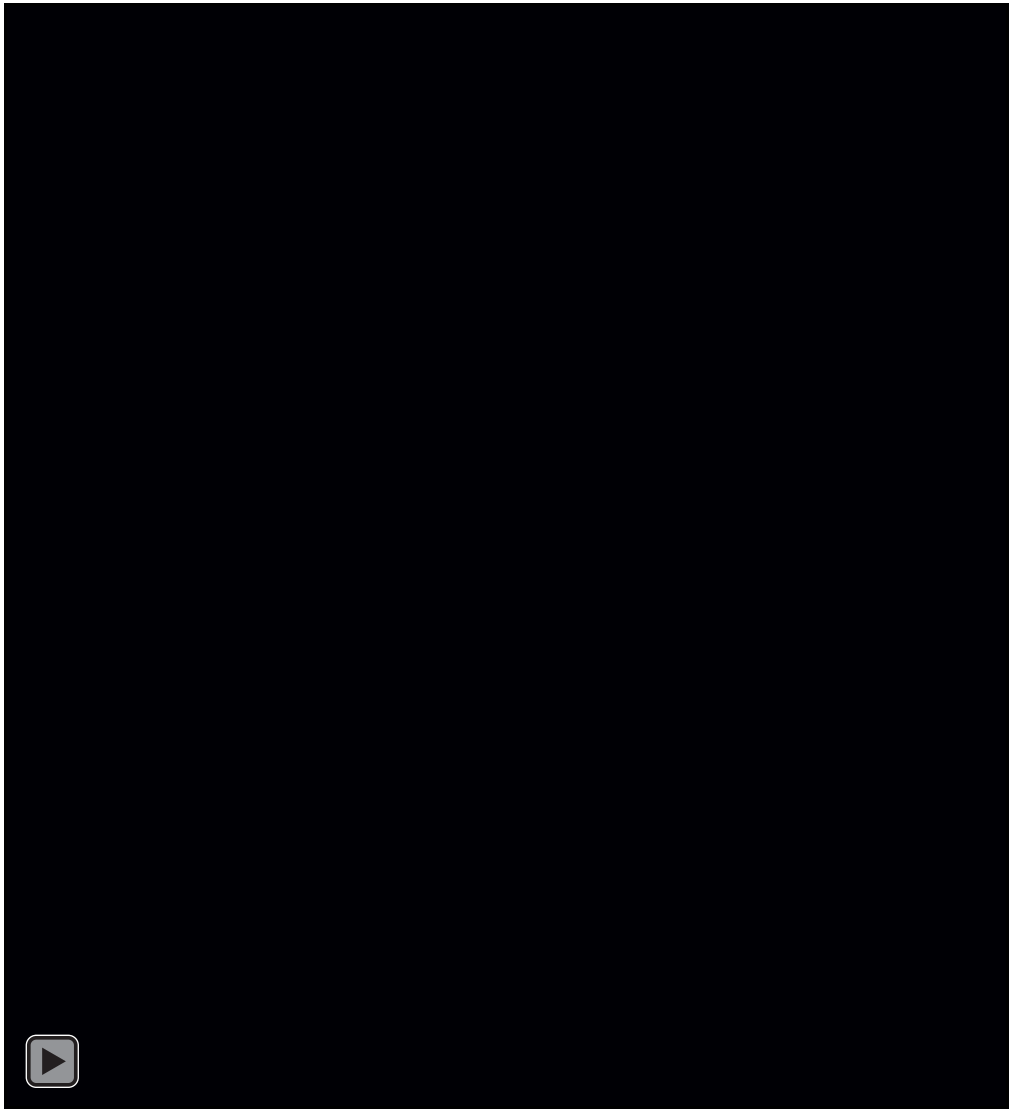

Possible names:

- Tapping Mode
- Amplitude Modulation AFM
- Semicontact Mode
- Intermittent Contact Mode
- AC-Mode
- Non-Contact Mode
- etc…

Morphological studies of RADA-16-I and RLDL-16-I fibrils

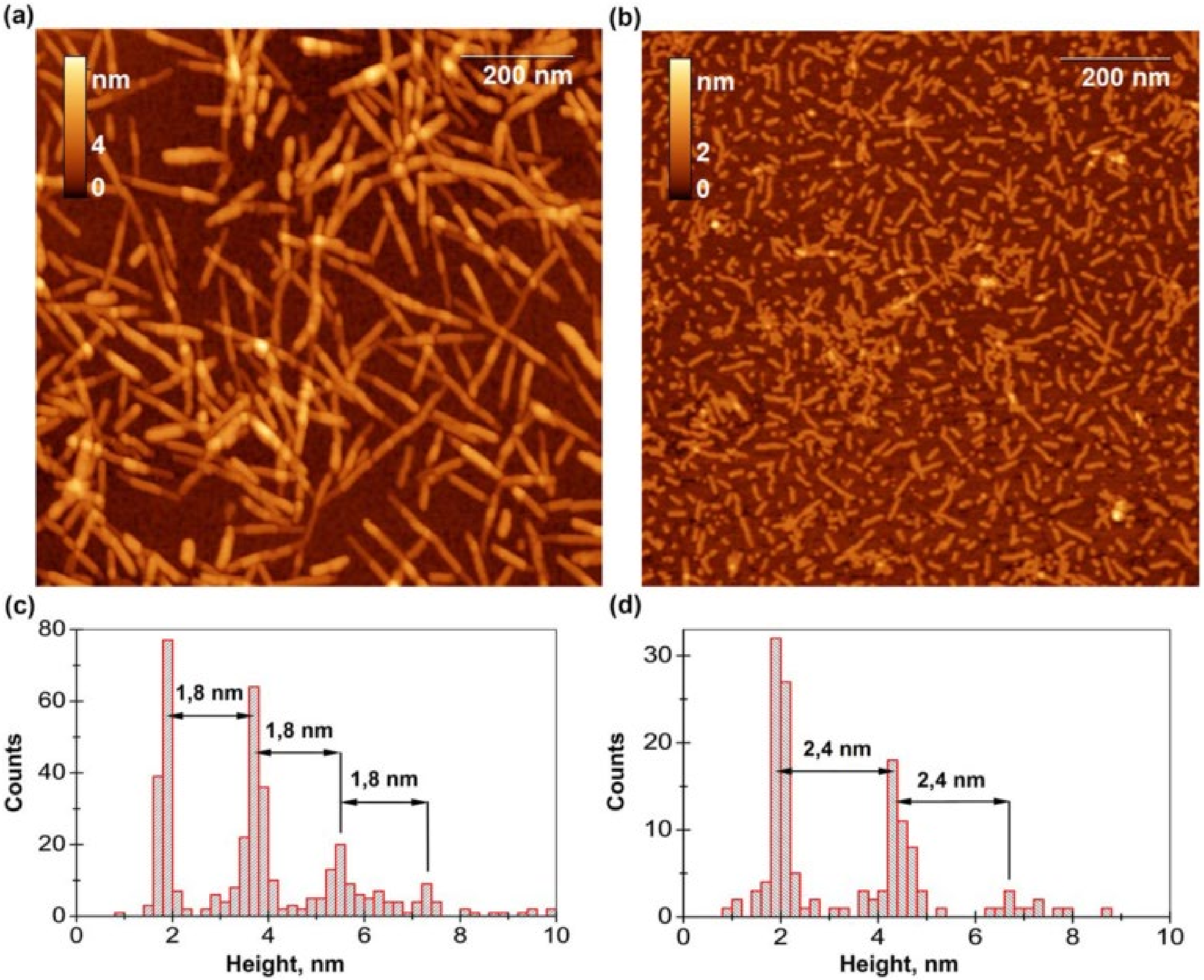

AFM images of RADA-16-I and RLDL-16-I fibrils. (a) AFM image of RADA-16-I fibrils deposited on mica, (b) AFM image of RLDL-16-I fibrils deposited on mica (c) Histogram of RADA-16-I fibrils height distribution showing 1.8 nm gap between the peaks, (d) histogram of RLDL-16-I fibrils height distribution showing 2.4 gap between the peaks

D. Bagrov, Y. Gazizova, V. Podgorsky, I. Udovichenko, A. Danilkovich, K. Prusakov and D. Klinov, "Morphology and aggregation of RADA-16-I peptide Studied by AFM, NMR and molecular dynamics simulations", *Biopolymers*, vol. 106, no. 1, pp. 72-81, 2016.

Studies of silver-coated DNA molecules (E-DNA)

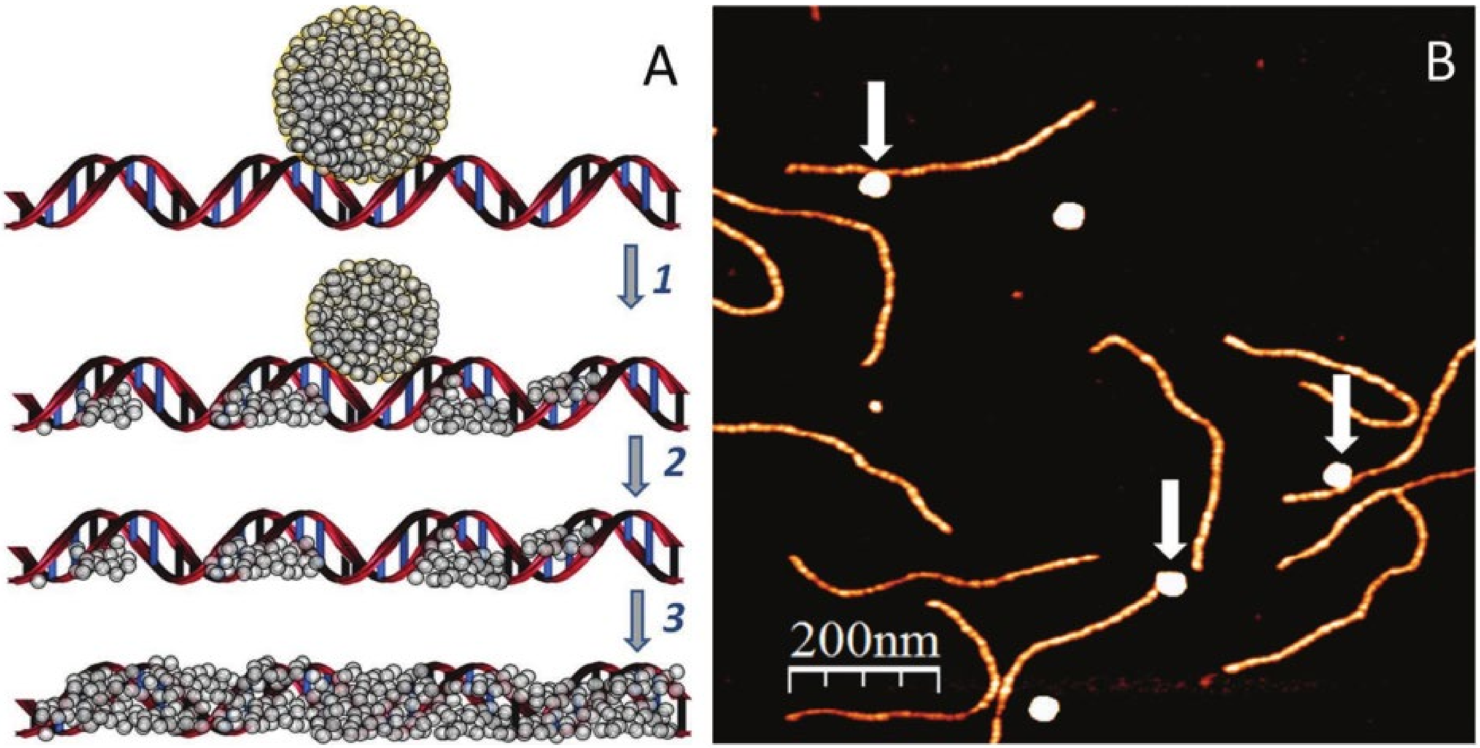

Tentative scheme of A) E-DNA formation and B) AFM imaging of an intermediate stage of E-DNA formation. A) (1) The AgNP binds to DNA and donates its atoms to the nucleic acid. As a result, silver atoms and few atoms clusters are positioned within or on the DNA molecules. (2) The NP dissociates, leaving some of its atoms bound to the DNA. (3) A number of binding–dissociation cycles yield E-DNA. B) The DNA was incubated with AgNPs for 20 h and imaged by AFM. AgNPs bound to the DNA molecules are indicated by the arrows.

Eidelshtein, G., Fardian-Melamed, N., Gutkin, V., Basmanov, D., Klinov, D., Rotem, D., Levi-Kalisman, Y., Porath, D. & Kotlyar, A. DNA-Metalization: Synthesis and Properties of Novel Silver-Containing DNA Molecules (Adv. Mater. 24/2016). *Advanced Materials* 28, 4944-4944 (2016).

AFM studies of patterned hydrogel film

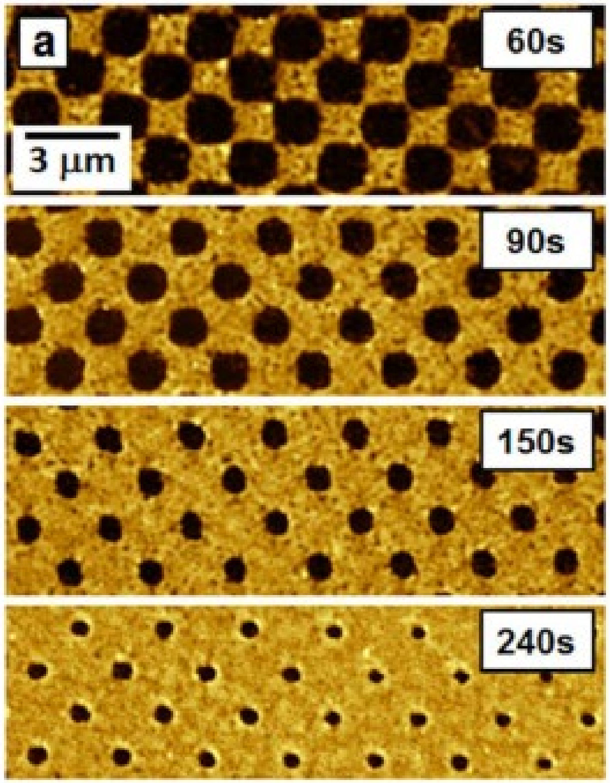

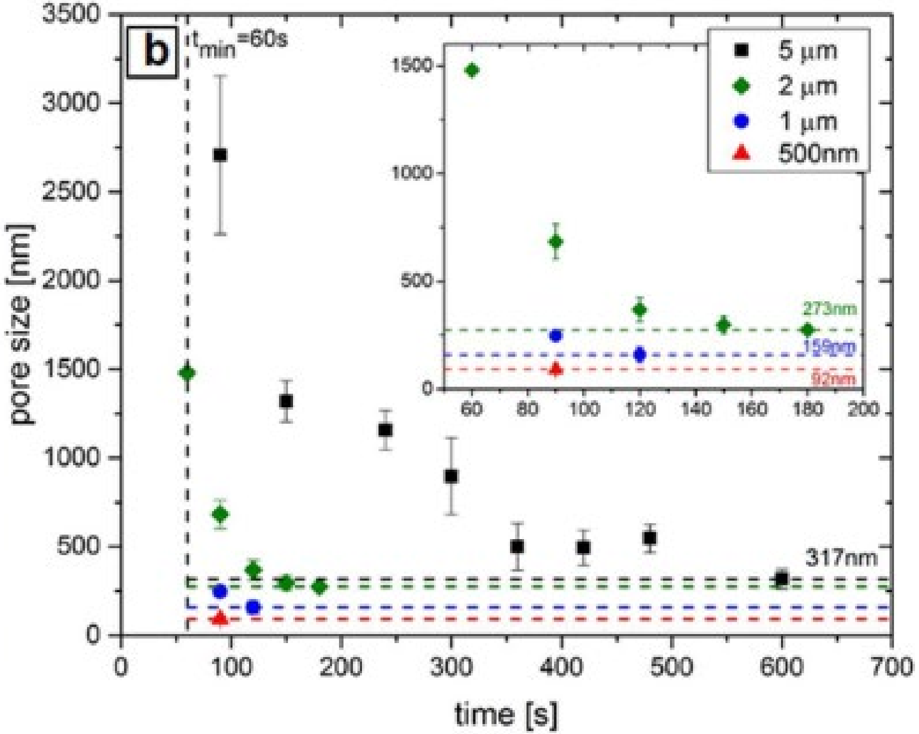

(a) AFM micrographs of the structured poly(NIPAm-co-10%MABP) + DR1 hydrogel film with a 2 µm period for different irradiation times. The pore diameter decreases and the pore spacing increases with increasing irradiation time. The depth of the pores is about 280 nm. (b) The dependence of the pore size on irradiation time at different periodicities of the interference pattern.

Jelken, J., Pandiyarajan, C., Genzer, J., Lomadze, N. & Santer, S. Fabrication of Flexible Hydrogel Sheets Featuring Periodically Spaced Circular Holes with Continuously Adjustable Size in Real Time. *ACS Applied Materials & Interfaces* 10, 30844-30851 (2018).

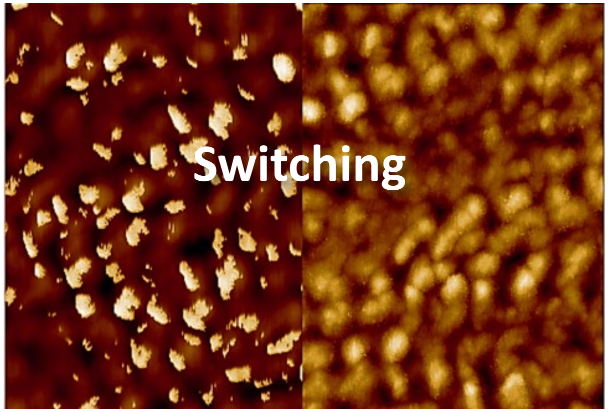

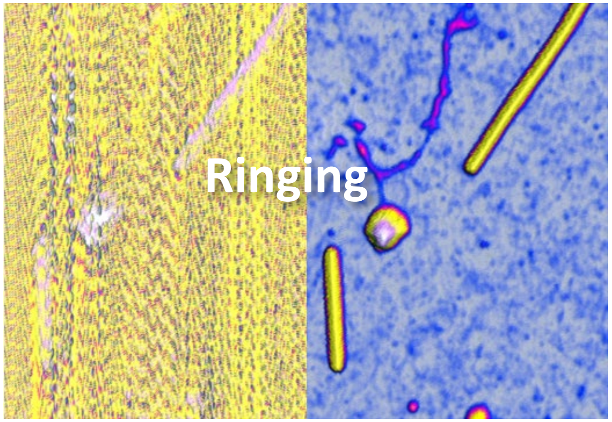

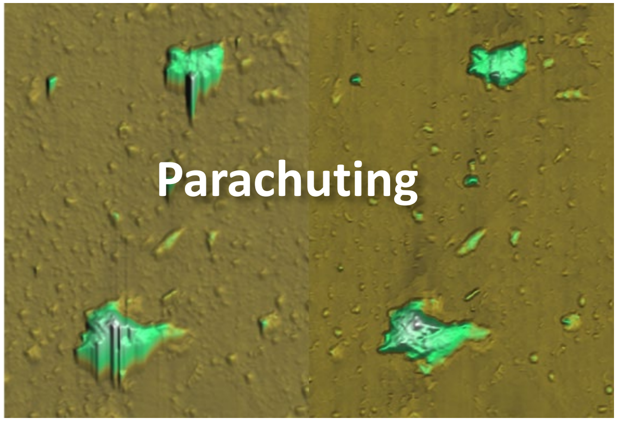

ScanT™

Straightforward for beginners

Helpful for experts

QNM with Force-Distance Curves

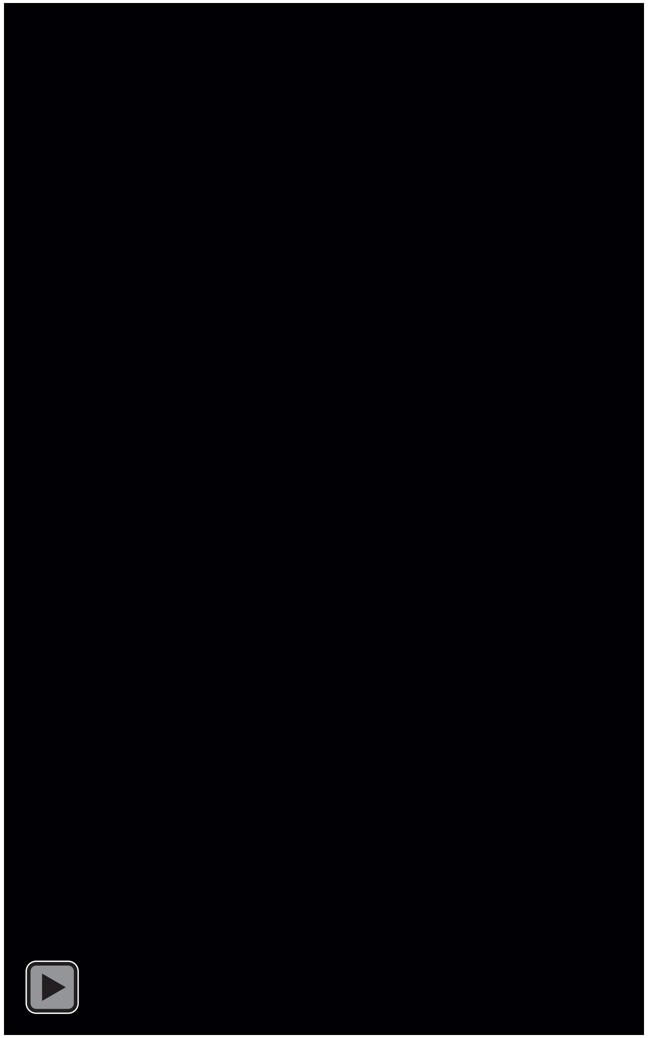

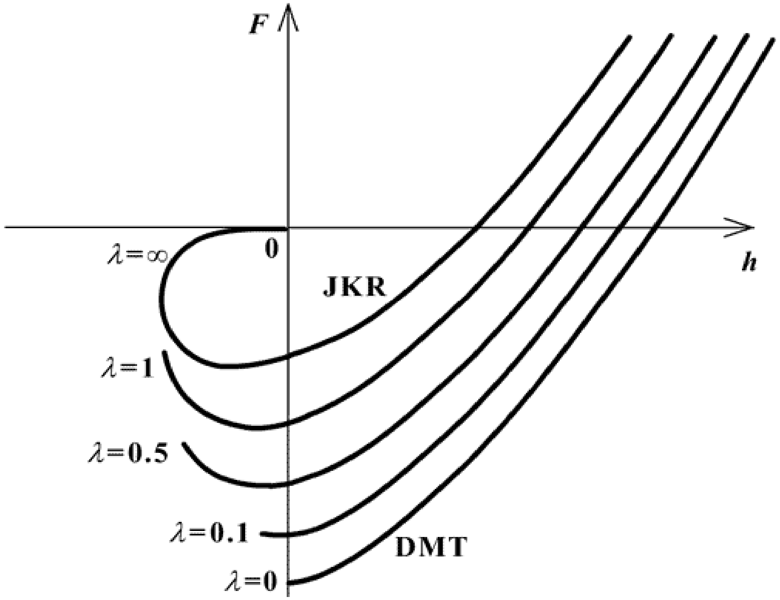

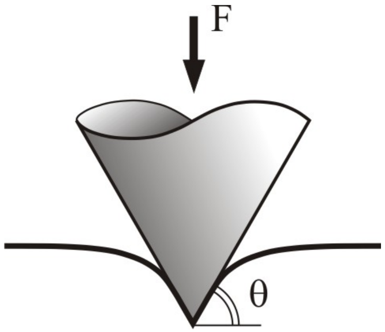

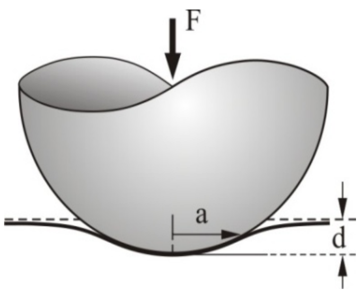

Mechanical studies of brown recluse spider silk

Mechanical studies of Brown Recluse Spider silk

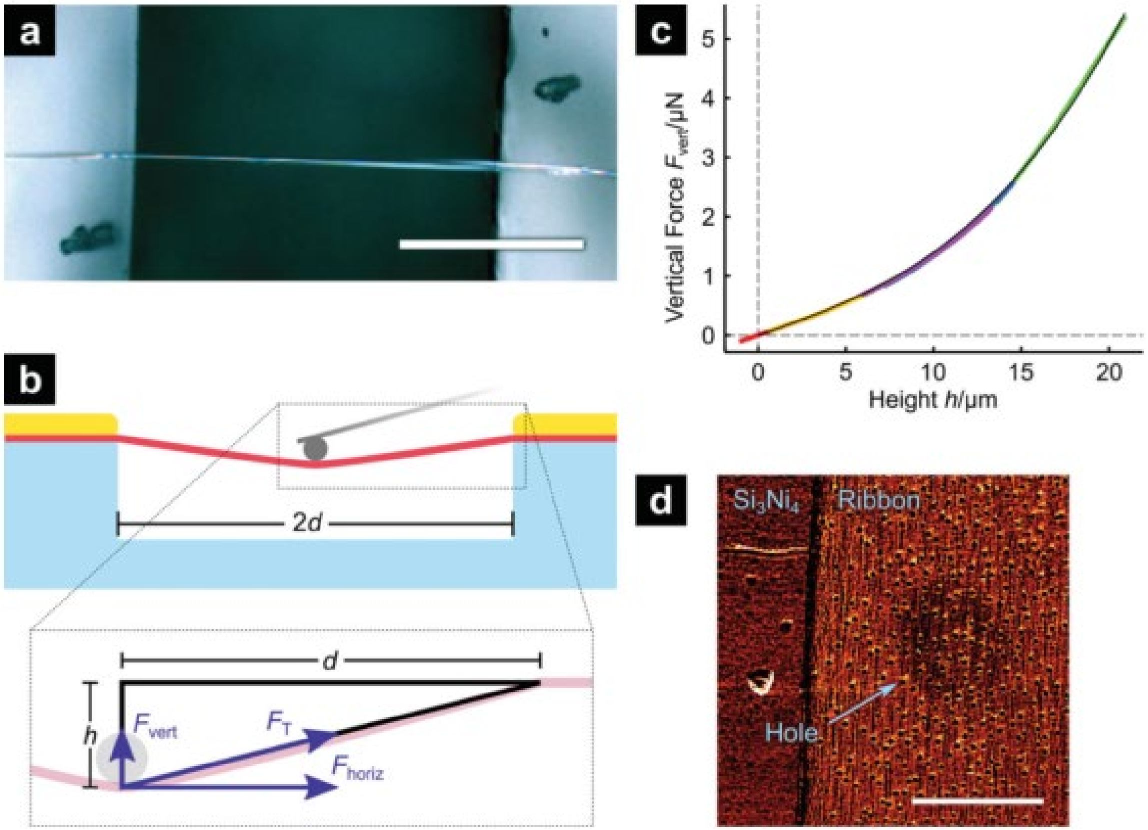

a) Top view of the mechanical testing setup (optical micrograph). Scale bar: 200 μ m. b) Schematic of the setup: a Loxosceles fiber (rose) was suspended over a gap in a glass substrate (light blue) and secured with cyanoacrylate glue (amber). A blunted AFM probe (grey) strained the silk via vertical defl ection, while simultaneously measuring the vertical component F vert of the fiber tensile force F T as a function of the probe indentation height h.

c) Obtained force curves (various colors) and the fitted model (black). d) AFM tapping-mode phase image of a silk ribbon suspended over a 1 μ m-diameter hole in a silicon nitride substrate. The ribbon covers the hole and can sustain forces exerted by the AFM probe. Phase imaging reveals the position of the hole since the ribbon deflects in the suspended area (scale bar: 1 μ m).

H. Schniepp, S. Koebley and F. Vollrath, "Brown Recluse Spider's Nanometer Scale Ribbons of Stiff Extensible Silk", *Advanced Materials*, vol. 25, no. 48, pp. 7028-7032, 2013.

Mechanical studies of Brown Recluse Spider silk

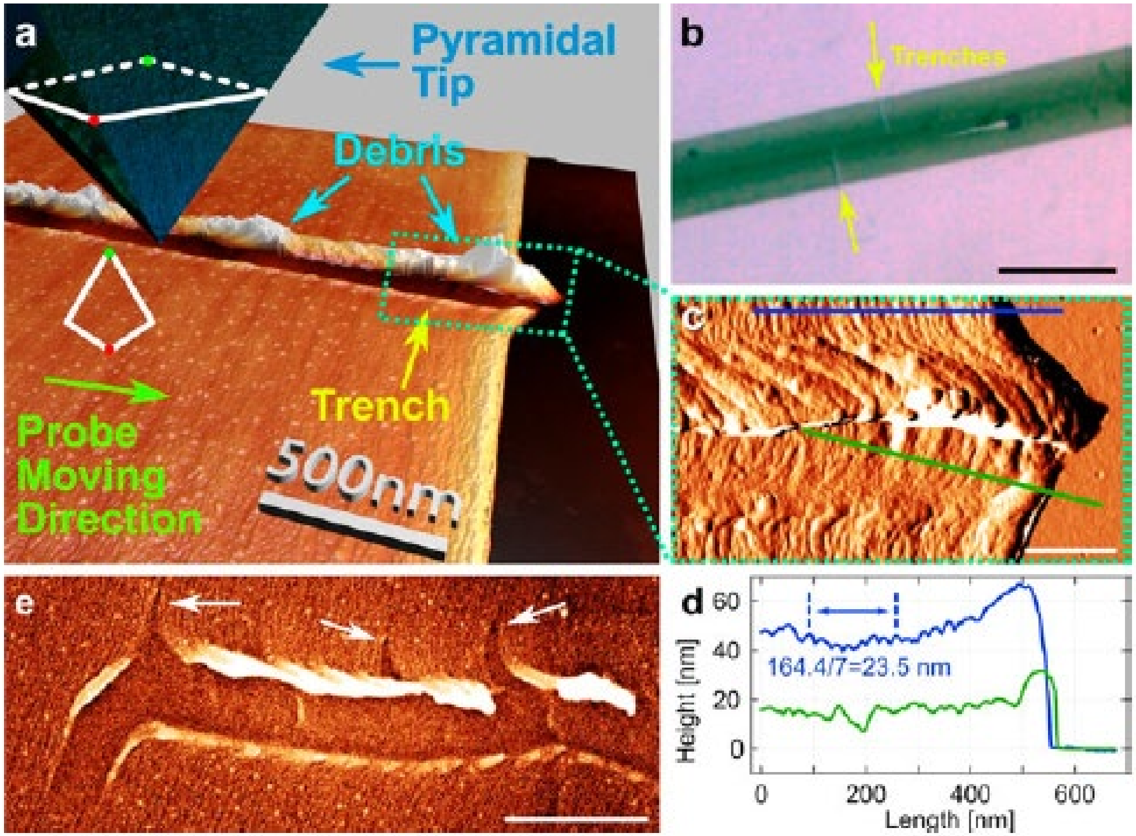

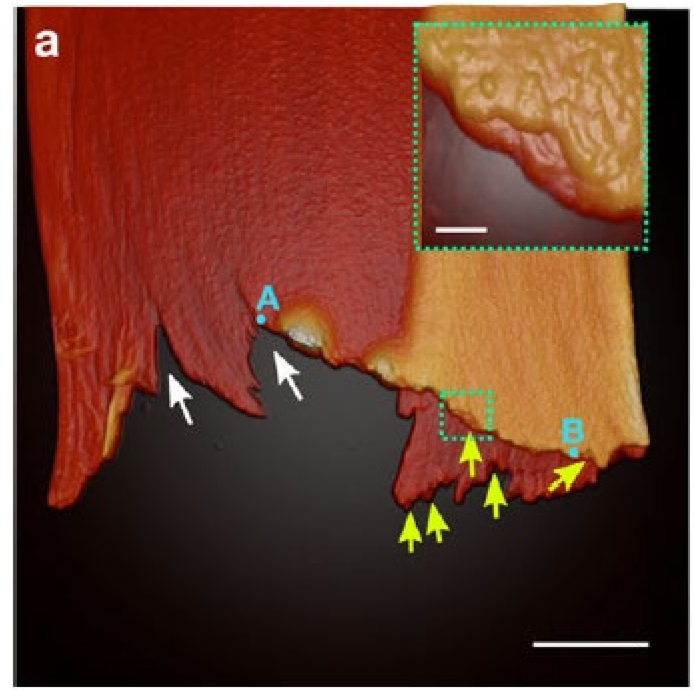

Breaking strength of a single nanofibril is ~120 nN

Wang, Q. & Schniepp, H. Strength of Recluse Spider's Silk Originates from Nanofibrils. *ACS Macro Letters* 7, 1364-1370 (2018).

NT-MDT Spectrum Instruments

Non-Resonance Oscillatory Mode (HybriD™ Mode)

•HybriD mode (HD mode) – scanning technique based on fast force-distance curves measurements with real-time processing of the tip response.

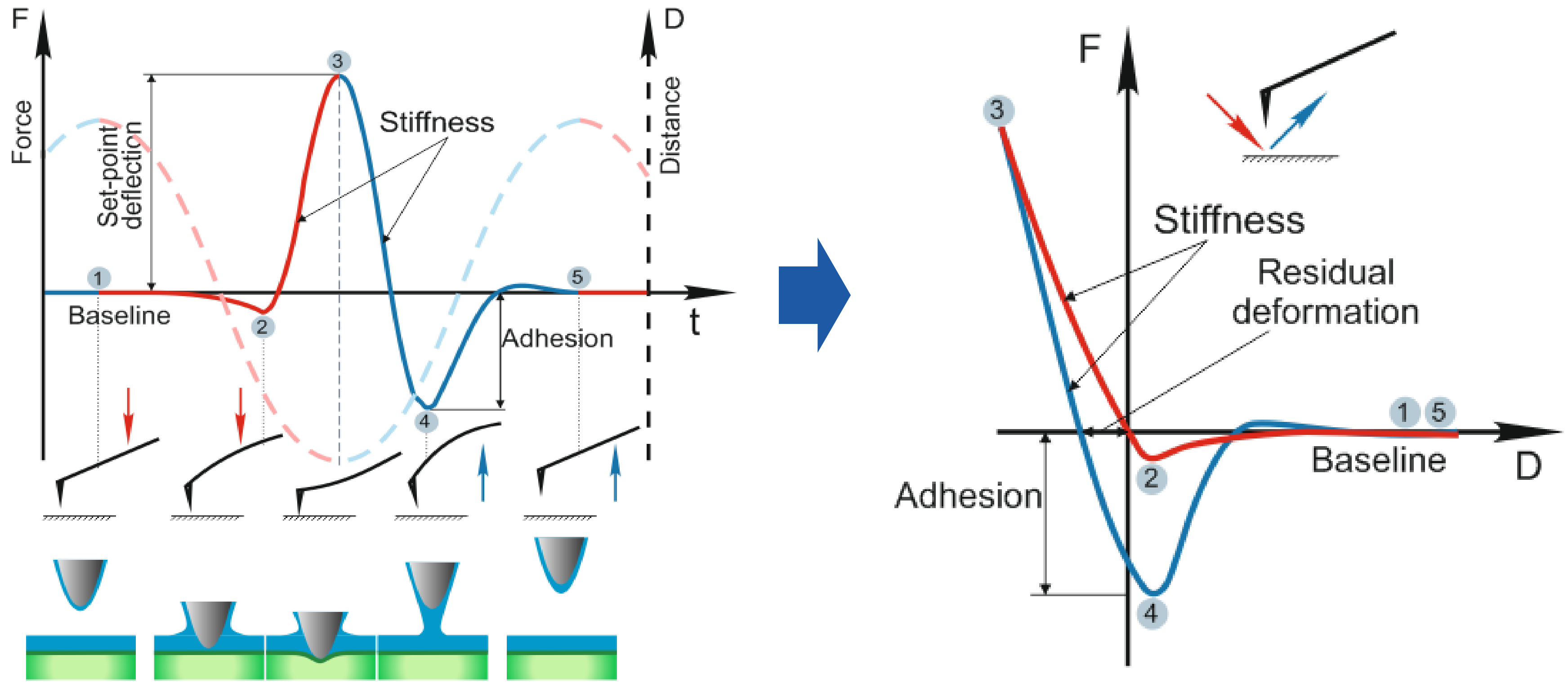

S. Magonov, S. Belikov, J. D. Alexander, C. G. Wall, S. Leesment, and V. Bykov, “Scanning probe based apparatus and methods for low-force profiling of sample surfaces and detection and mapping of local mechanical and electromagnetic properties in non-resonant oscillatory mode,” US9110092B1.

Morphological and Mechanical Studies of Polymer Blends

Topography

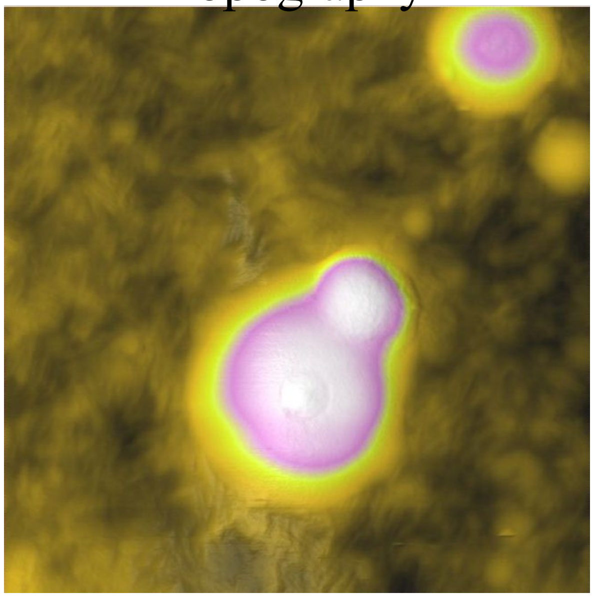

Adhesion

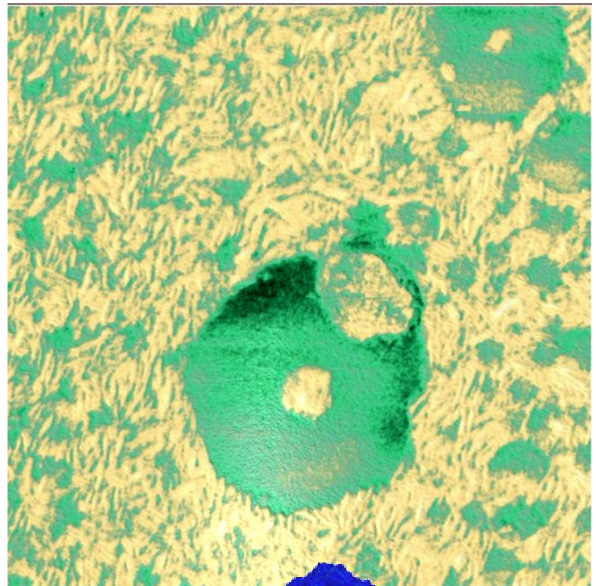

E Modulus

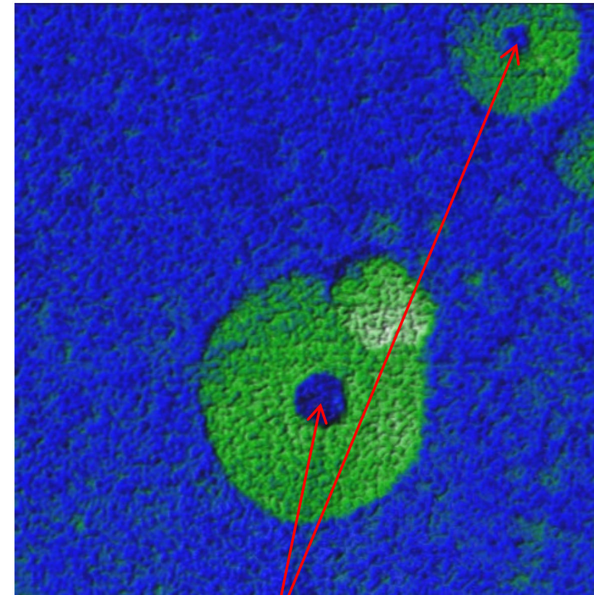

Polyethylene blobs on polystyrene spheres

Scan Size:
3×3 μm

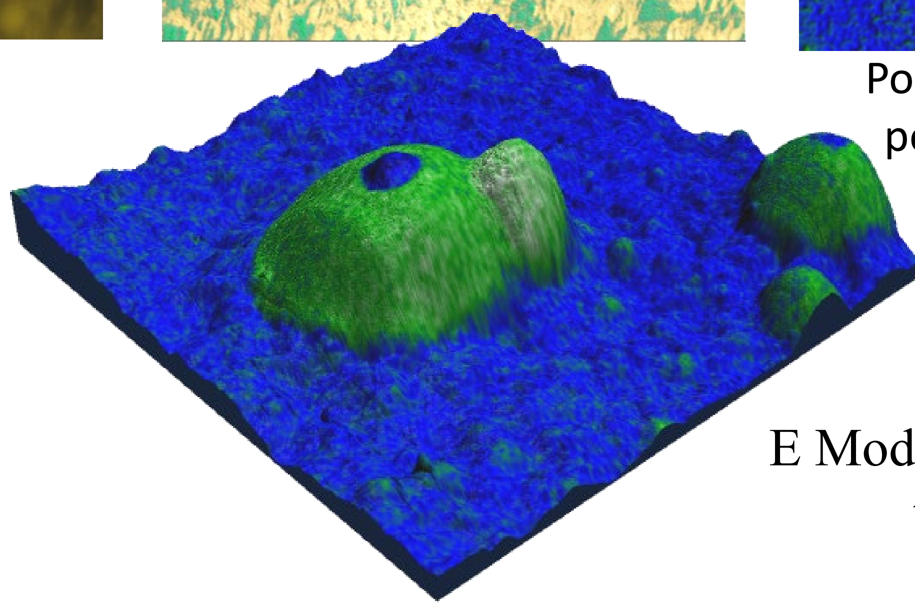

E Modulus overlaid over topography

HD Studies in Vacuum

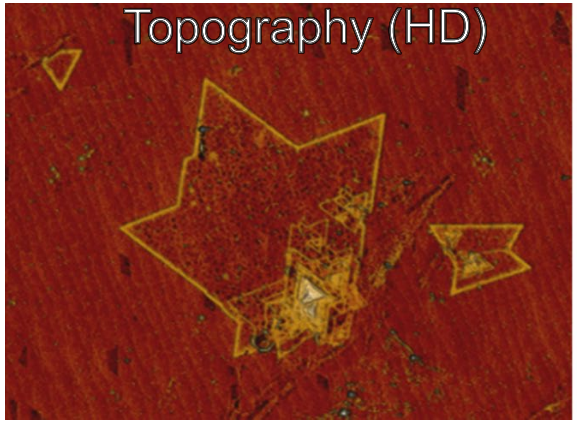

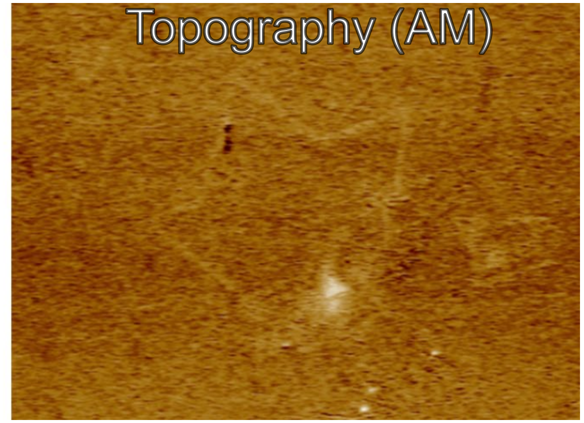

WS_2 monolayers grown on epitaxial graphene measured in vacuum with use of HD and AM modes. The influence of electrostatic forces is demonstrated. Scan size: 14×14 µm

Vacuum setup of NTEGRA AFM

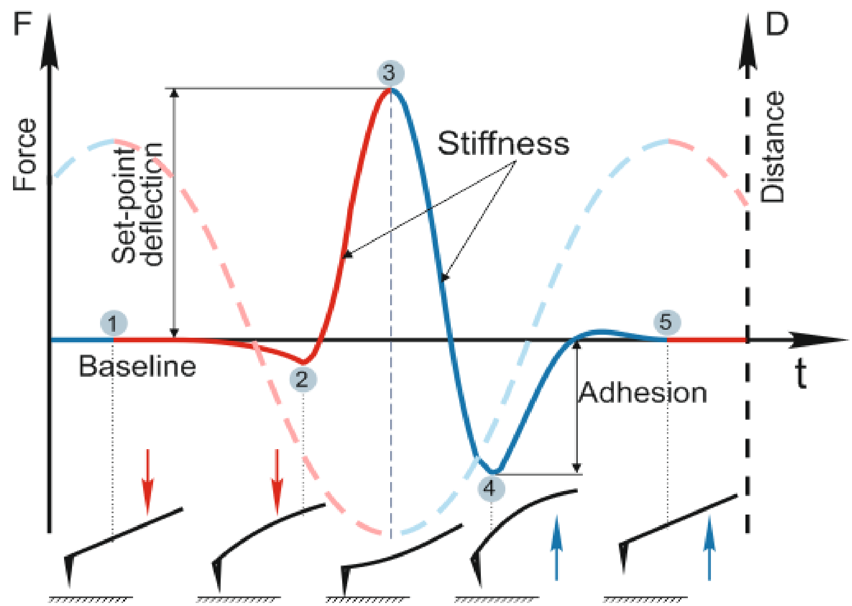

Sample courtesy:
Dr. Cristina Giusca (NPL, UK),
Prof. Mauricio Terrones (PSU, USA)

Set-point calculation principle eliminating electrostatic force gradient

NT-MDT Spectrum Instruments

Conductive AFM (C-AFM)

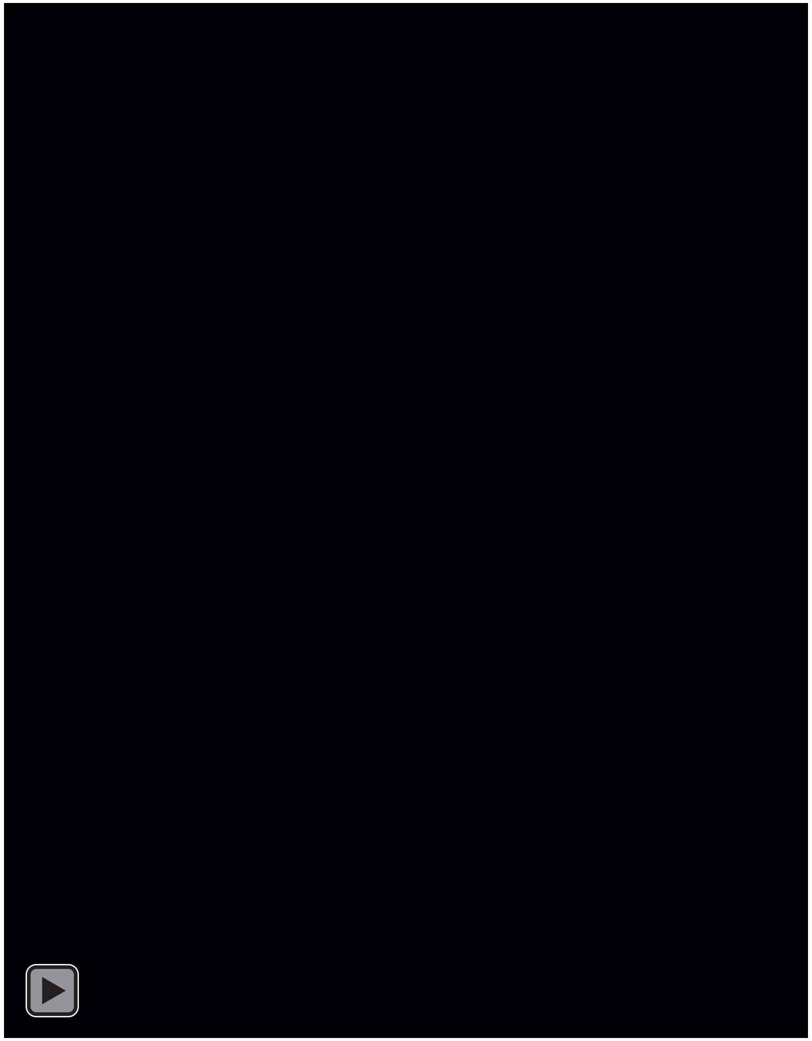

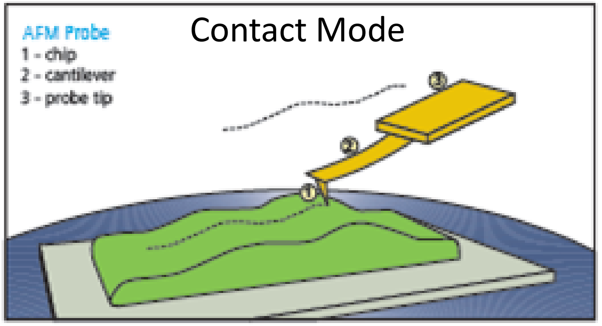

High resolution characterization of grain boundaries in Cu2ZnSnSe4 solar cells

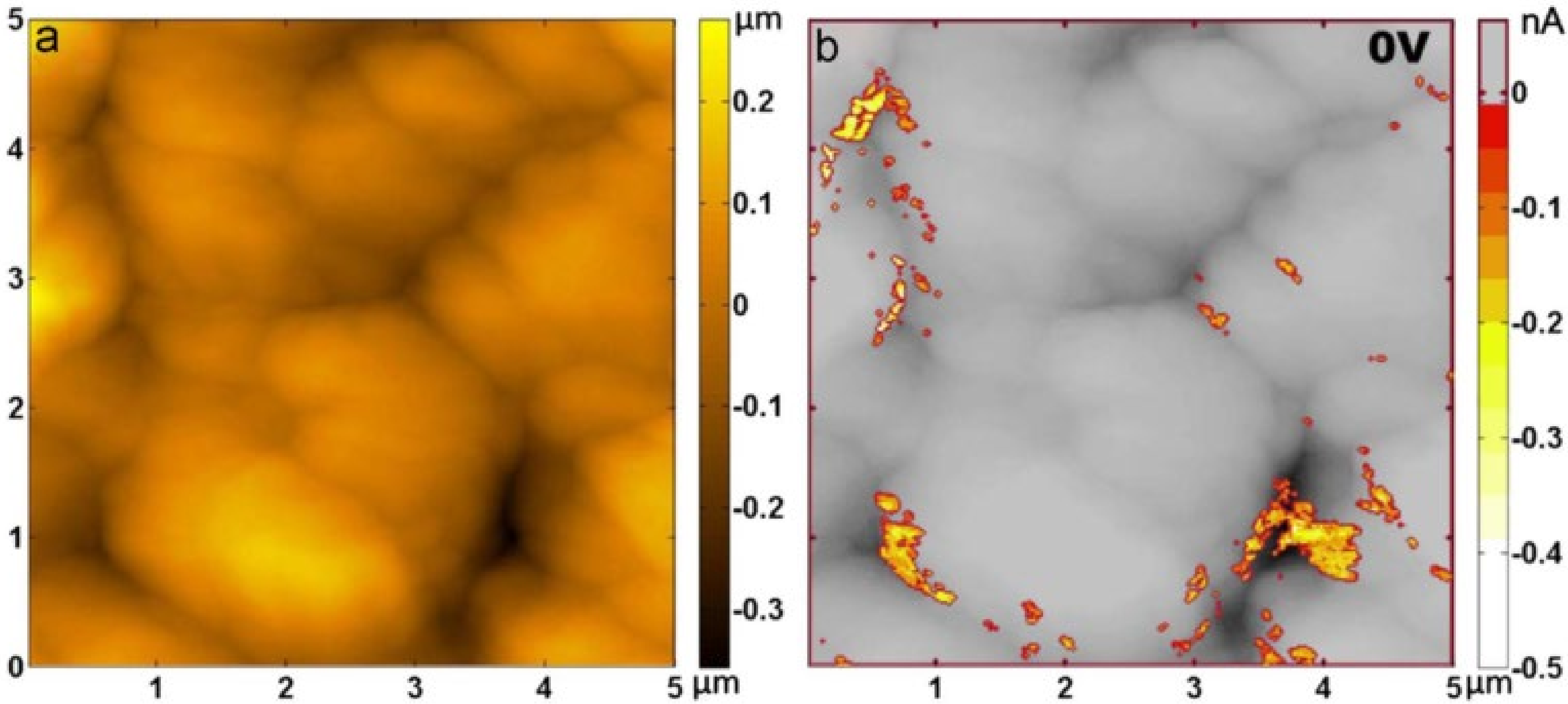

(a) AFM topography of the top surface of a CZTSe device. (b) Zero biased photocurrent mapping, under illumination of a defocused 532 nm continuous wave laser with total power of 1mW. The photocurrent mapping is superimposed on the topography in (a) to illustrate the correlation between the position of the photo current and that of the GBs

M. Xu, B. Liu, G. Graham and X. Pan, "High resolution characterization of grain boundaries in Cu 2 ZnSnSe4 solar cells synthesized by nanoparticle selenization", *Solar Energy Materials and Solar Cells*, vol. 157, pp. 171-177, 2016.

NT-MDT Spectrum Instruments

HybriD Conductive AFM

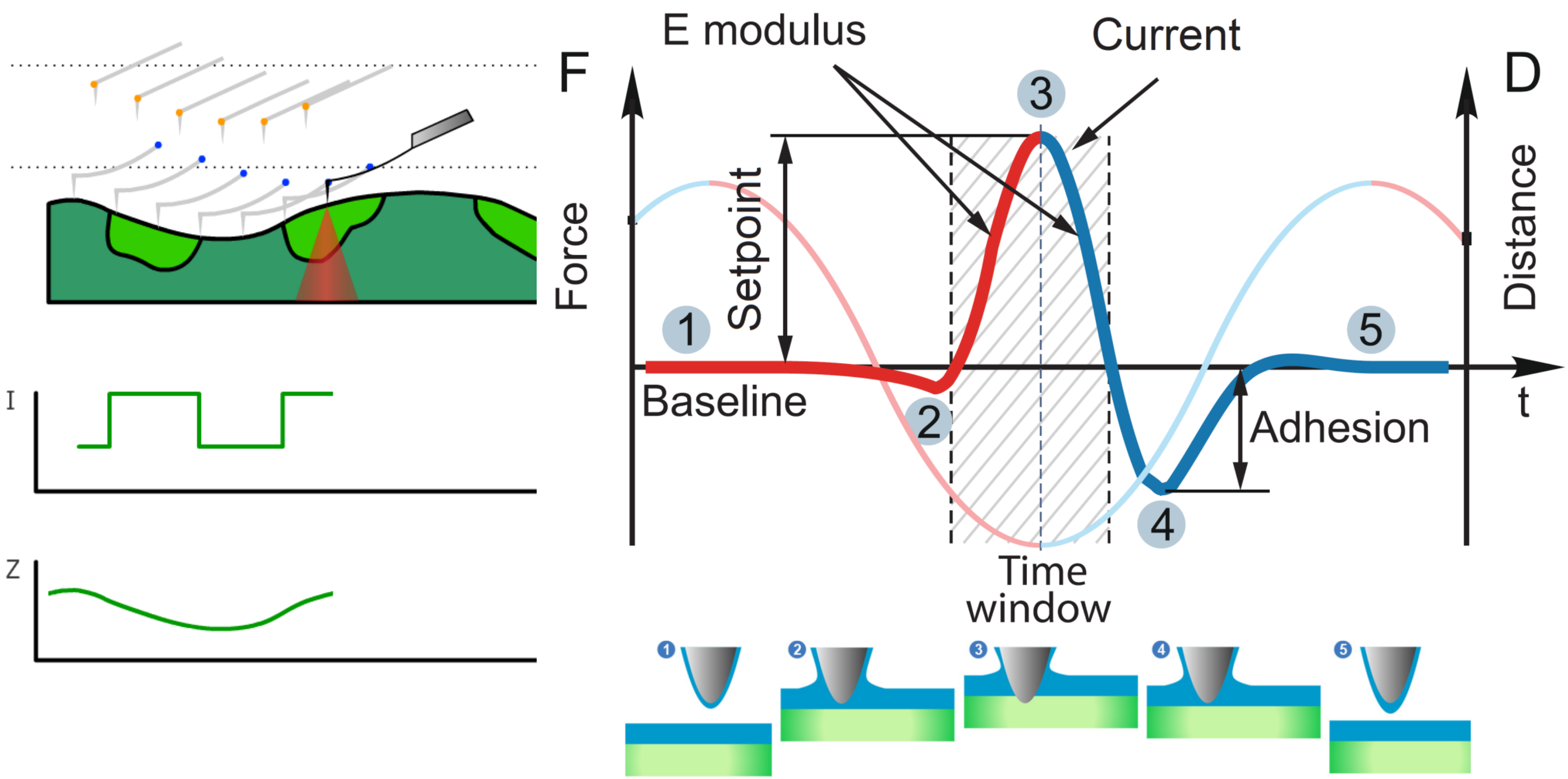

Conductive Studies of Silver Nanotubes

There is a gradient of current along the nanotube

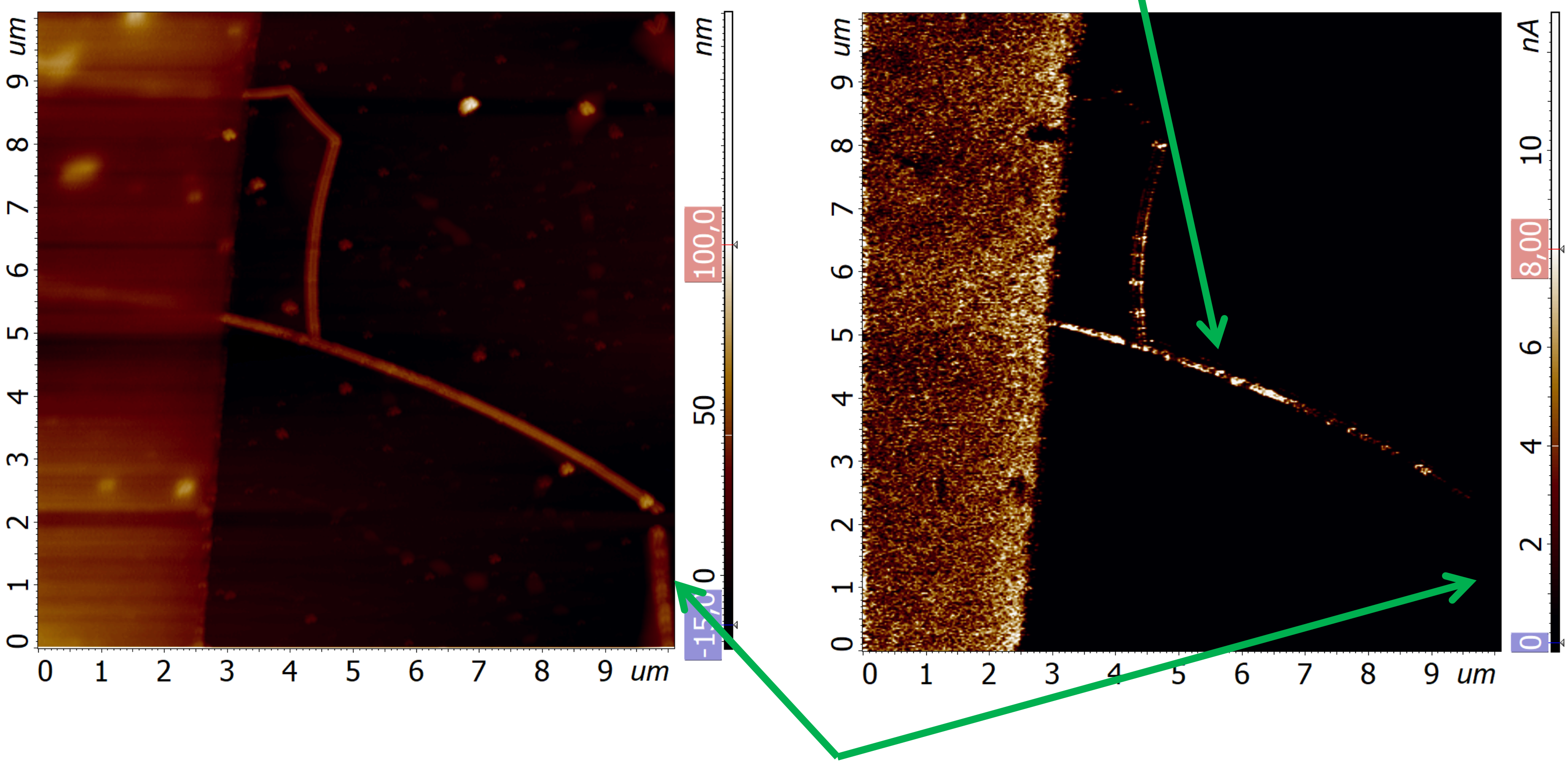

Nanotube is not connected to the electrode

Sample courtesy: Prof. D. Klinov, FMBA, Moscow, Russia

NT-MDT Spectrum Instruments

Conductive and Mechanical Studies of Nanotubes by HD-CAFM

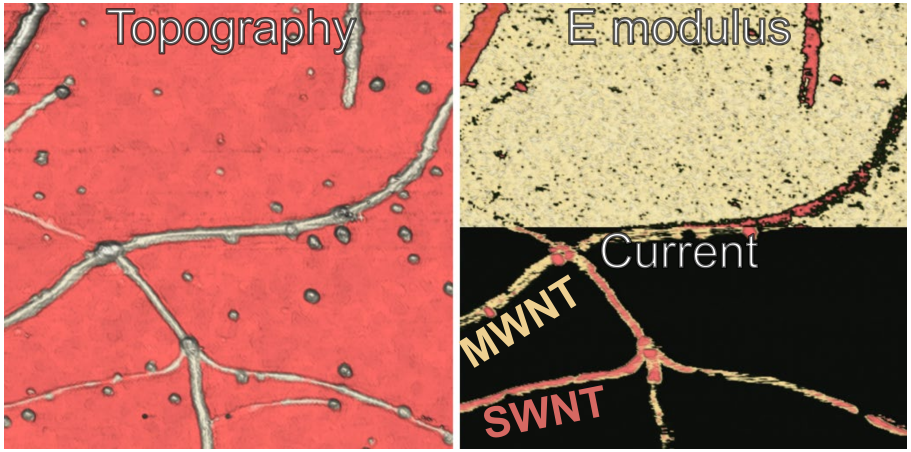

HD C-AFM study of carbon Nanotubes on Silicon.

Scan size: 1×1 µm.

Sample Courtesy: Dr. Irma Kuljanishvili, Saint Louis University, Department of Physics

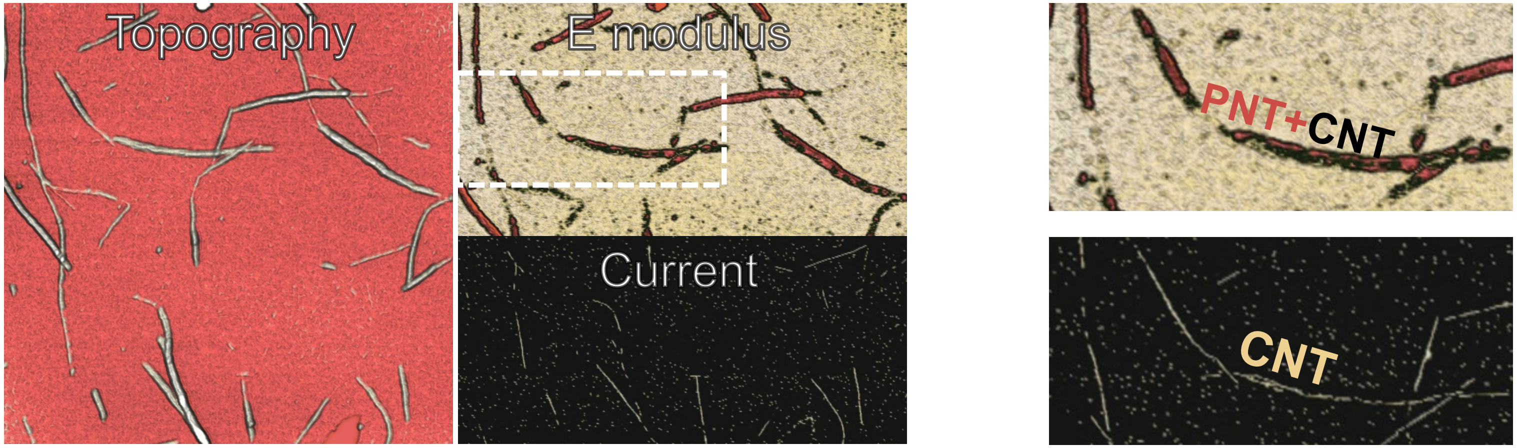

HD C-AFM study of coupled carbon and peptide Nanotubes. Sample courtesy: Dr. J. Montenegro, University Santiago de Compostela. Scan size: 3×3 µm[1].

[1] J. Montenegro, C. Vázquez-Vázquez, A. Kalinin, K.E. Geckeler, J.R. Granja, Coupling of carbon and peptide nanotubes, *J. Am. Chem. Soc.* 136 (2014) 2484–2491

Piezoresponse Force Microscopy (PFM)

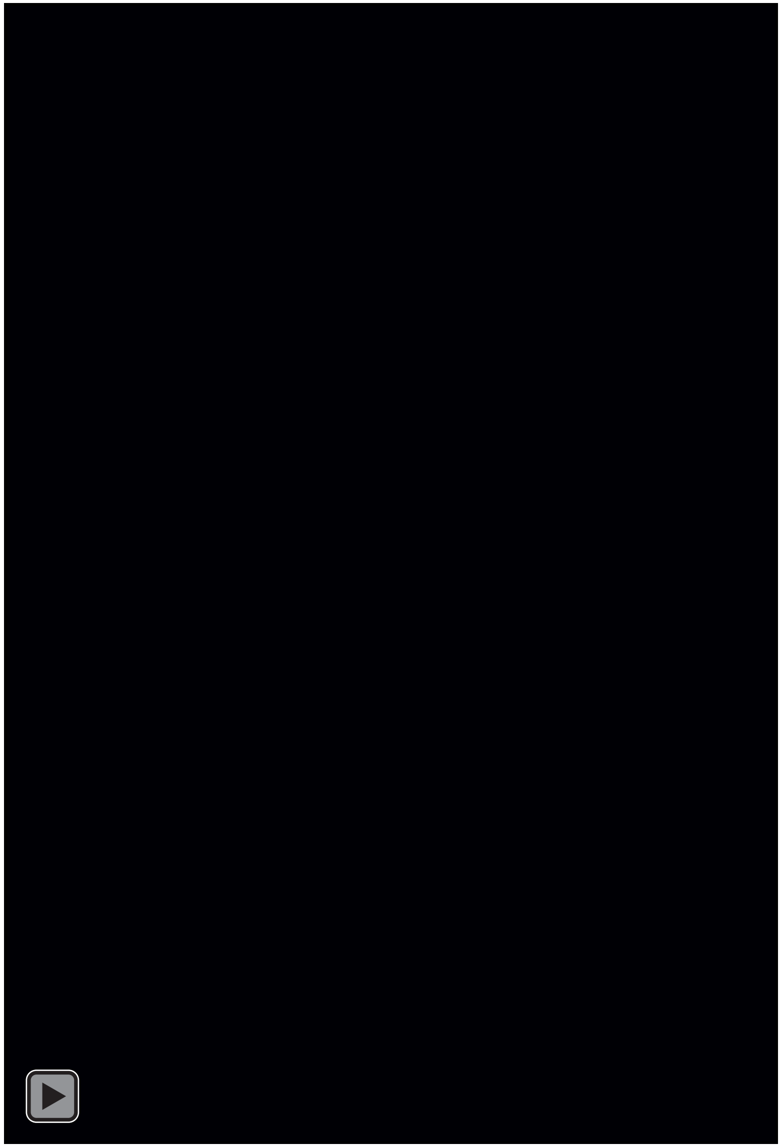

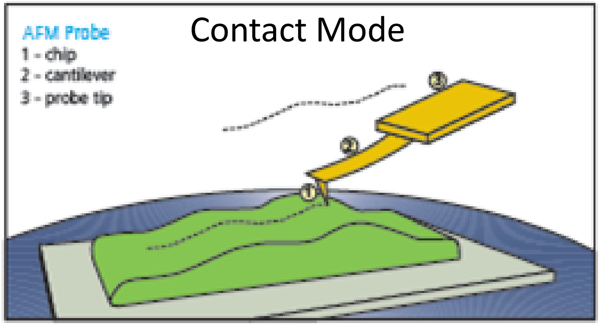

PFM studies of Bi0.9La0.1FeO3 ceramics

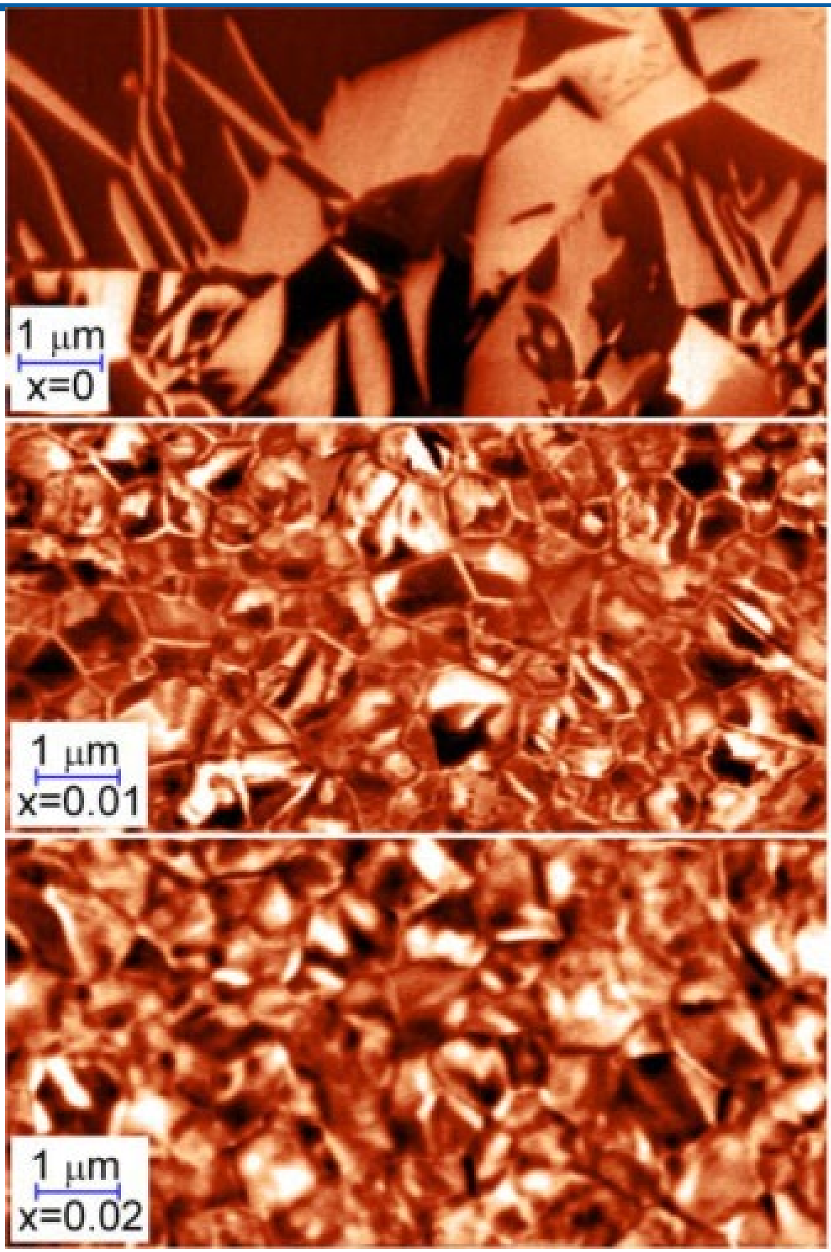

Vertical PFM images of the Bi0.9La0.1Fe1-xNbxO3+x ceramics. An A cos ϕ signal was recorded. Here, A is the amplitude of the measured vibration proportional to the effective longitudinal piezoelectric coefficient and ϕ is the phase shift determining the direction of polarization (the bright and dark regions correspond to polarization vectors directed to the free surface and to the bottom electrode, respectively)

PFM Studies confirm the effect of Effect of Nb doping

B. Stojadinović, B. Vasić, D. Stepanenko, N. Tadić, R. Gajić and Z. Dohčević-Mitrović, "Variation of electric properties across the grain boundaries in BiFeO3film", *Journal of Physics D: Applied Physics*, vol. 49, no. 4, p. 045309, 2015.

NT-MDT Spectrum Instruments

HD PFM

In HD PFM an AC voltage is applied to the conductive coating of the AFM cantilever when the tip comes in contact with the sample during each fast force spectroscopy cycle.

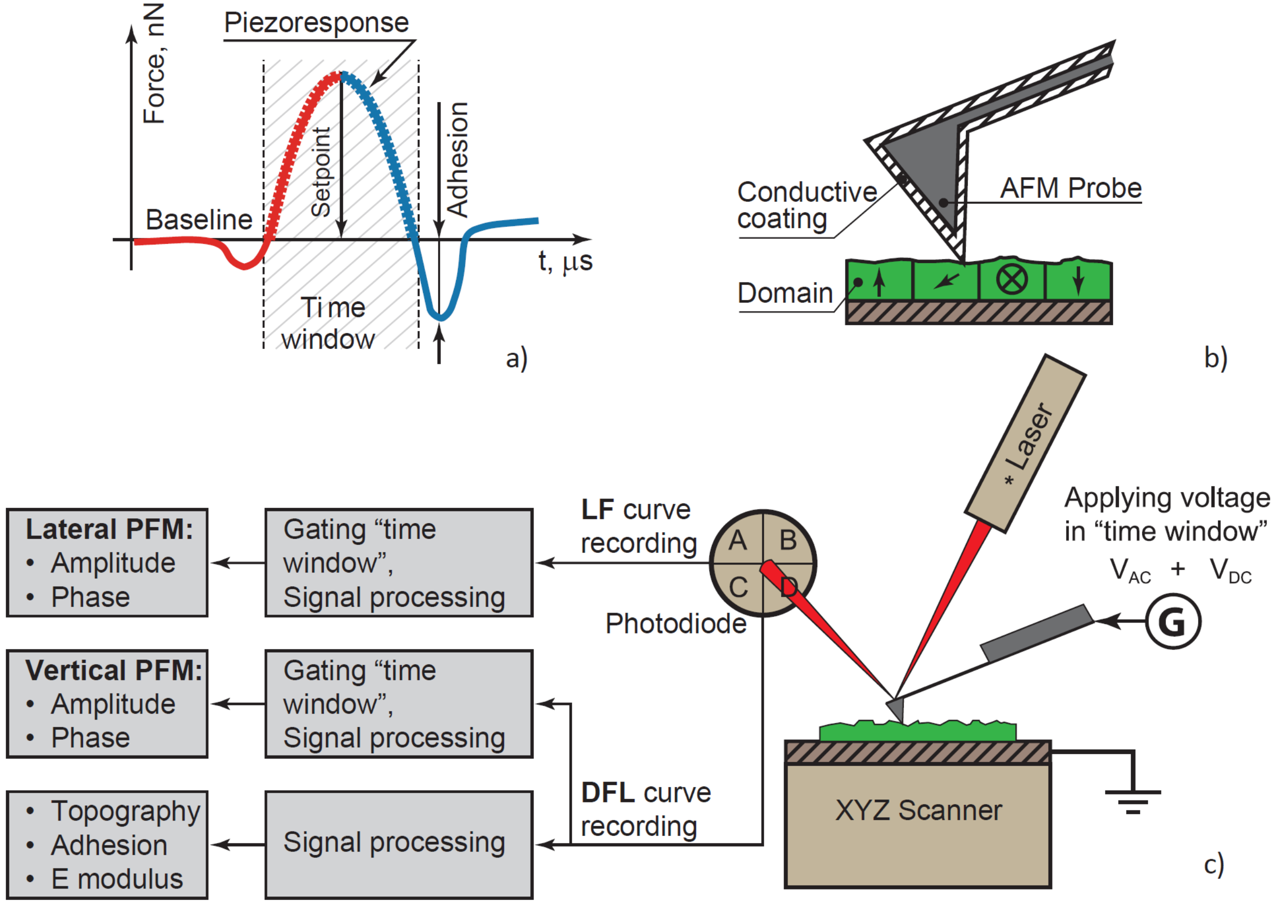

•*HD PFM working principle: a) an idealized temporal deflection curve during an*
•*oscillatory cycle, b) tip-sample interaction in “time window”, c) measurement scheme*

NT-MDT Spectrum Instruments

Electromechanical studies of diphenylalanine peptide nanotubes

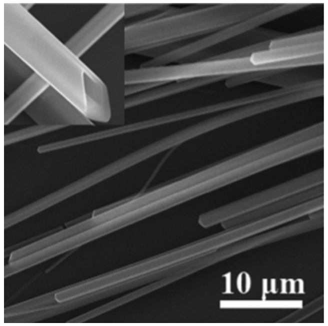

d_{15} = 60 pm/V[1]
E modulus = 19÷32 GPa

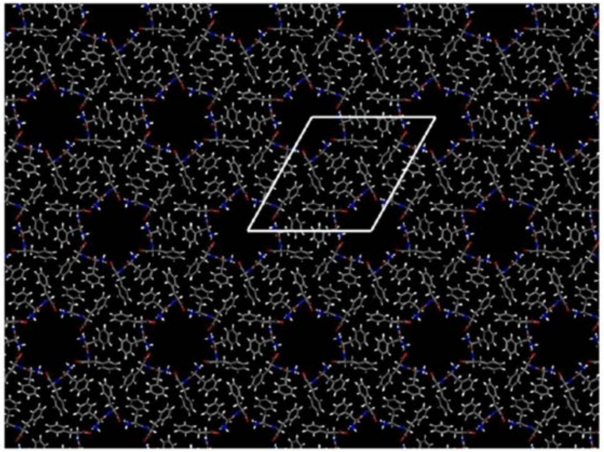

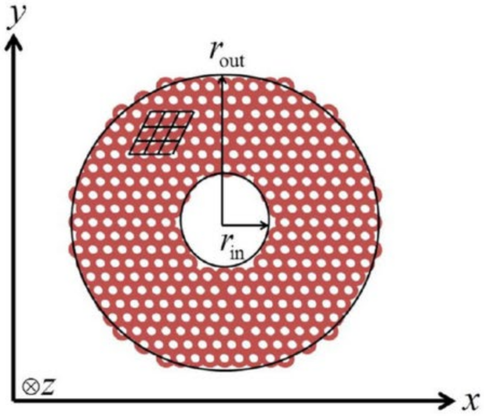

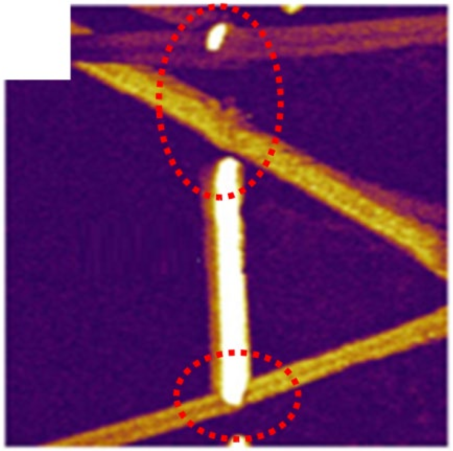

- Molecular structure of diphenylalanine peptide nanotubes[1]
- Contact PFM image[2]

[1]Kholkin, A., Amdursky, N., Bdikin, I., Gazit, E., & Rosenman, G. (2010) ACS nano, 4(2), 610-614.
[2]Ivanov, M., Kopyl, S., Tofail, S. A., Ryan, K., Rodriguez, B. J., Shur, V. Y., & Kholkin, A. L. (2016) In Electrically Active Materials for Medical Devices (pp. 149-166).

Electromechanical studies of diphenylalanine peptide nanotubes

For the first time HD PFM mode allowed non-destructive piezoresponse study of diphenylalanine peptide nanotubes – a very prospective material for biomedical applications.

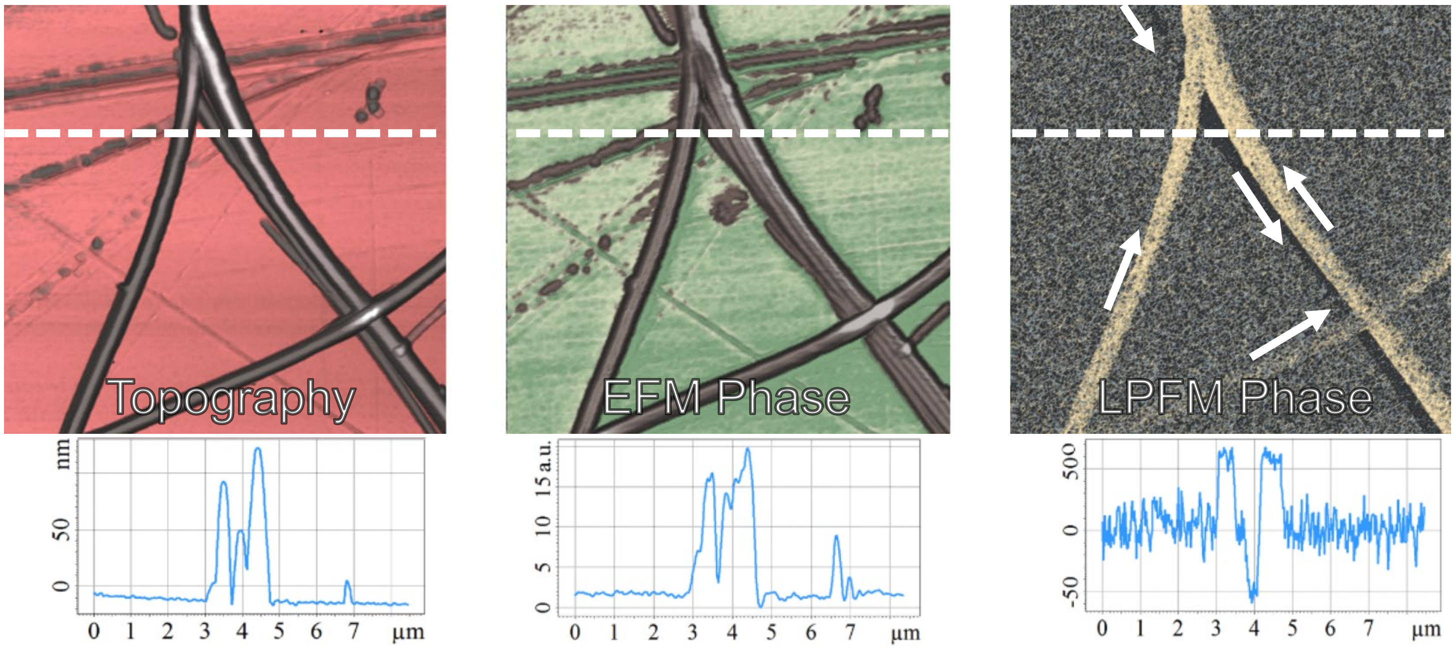

Non-destructive electromechanical study of diphenylalanine peptide nanotubes. Scan size: 8×8 µm, nanotubes diameter: 30÷150 nm.
Sample courtesy: Dr. A. Kholkin, University of Aviero

A. Kalinin, V. Atepalikhin, O. Pakhomov, A. Kholkin and A. Tselev, "An atomic force microscopy mode for nondestructive electromechanical studies and its application to diphenylalanine peptide nanotubes", *Ultramicroscopy*, vol. 185, pp. 49-54, 2018.

Electromechanical studies of diphenylalanine peptide nanotubes

- For the first time HD PFM mode allowed non-destructive piezoresponse study of diphenylalanine peptide nanotubes – a very prospective material for biomedical applications.

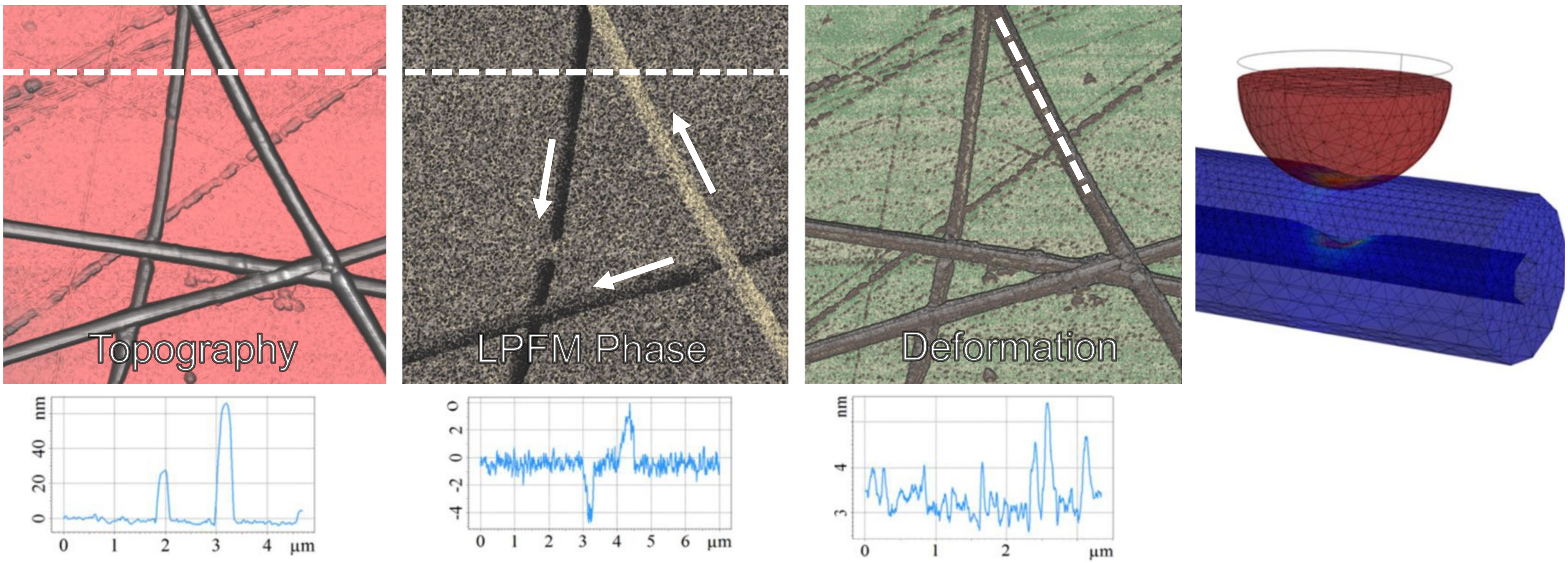

- Non-destructive electromechanical study of diphenylalanine peptide nanotubes. Scan size: 7×7 µm, nanotubes diameter: 70÷100 nm[1]. Sample courtesy: Dr. A. Kholkin, University of Aviero

A. Kalinin, V. Atepalikhin, O. Pakhomov, A. Kholkin and A. Tselev, "An atomic force microscopy mode for nondestructive electromechanical studies and its application to diphenylalanine peptide nanotubes", *Ultramicroscopy*, vol. 185, pp. 49-54, 2018.

In situ PFM studies under varying temperature

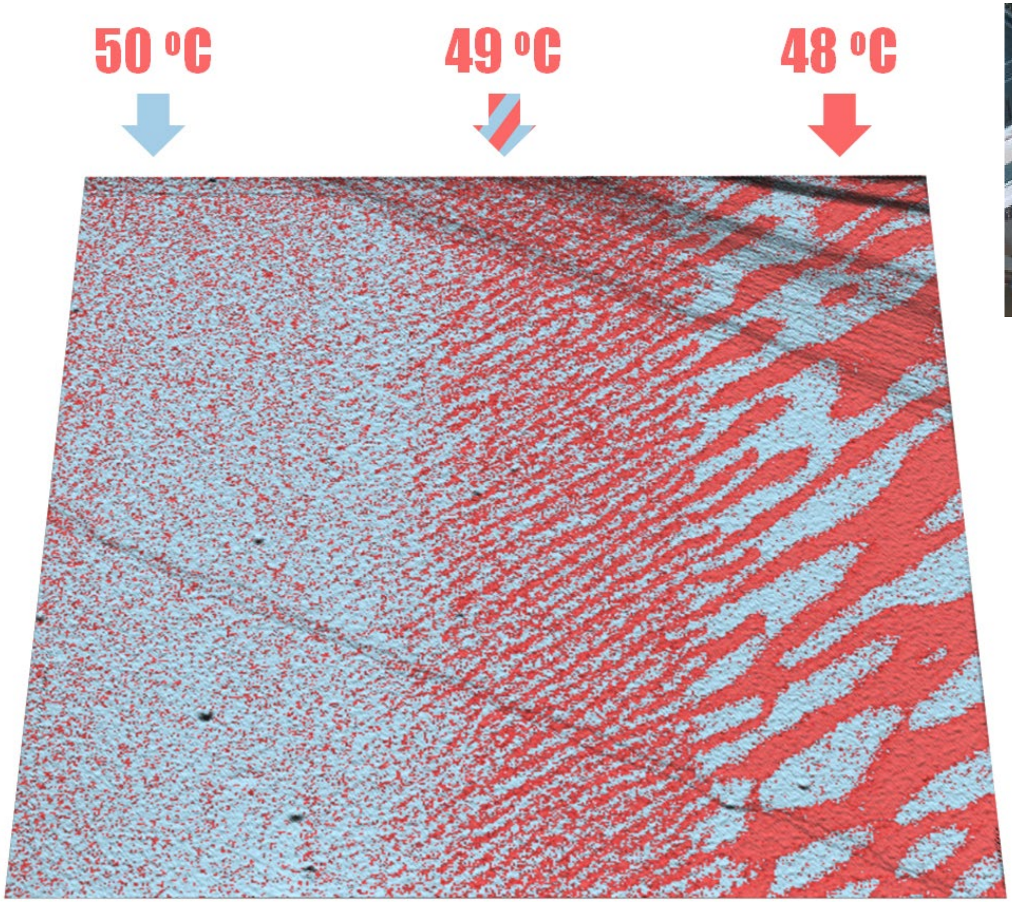

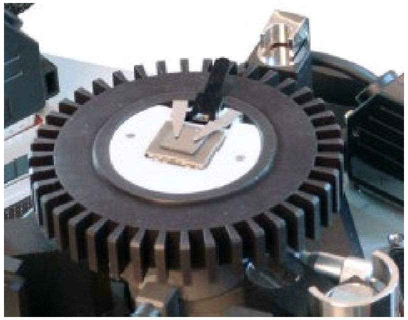

RT÷300 °C

-30÷120 °C

NT-MDT S.I. accessories for sample temperature control

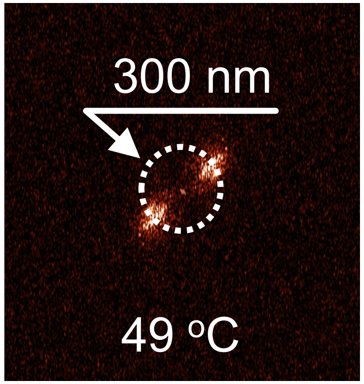

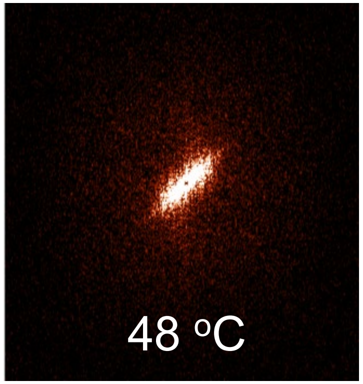

In-situ HD PFM study of second-order phase transition of triglycine sulfate crystal. Scan size 15×15 µm. Sample courtesy: Dr. R. Gainutdinov, IC RAS

HD PFM

Continuous PFM studies under variable temperature
>0.1 ^{o}C/sec temperature change

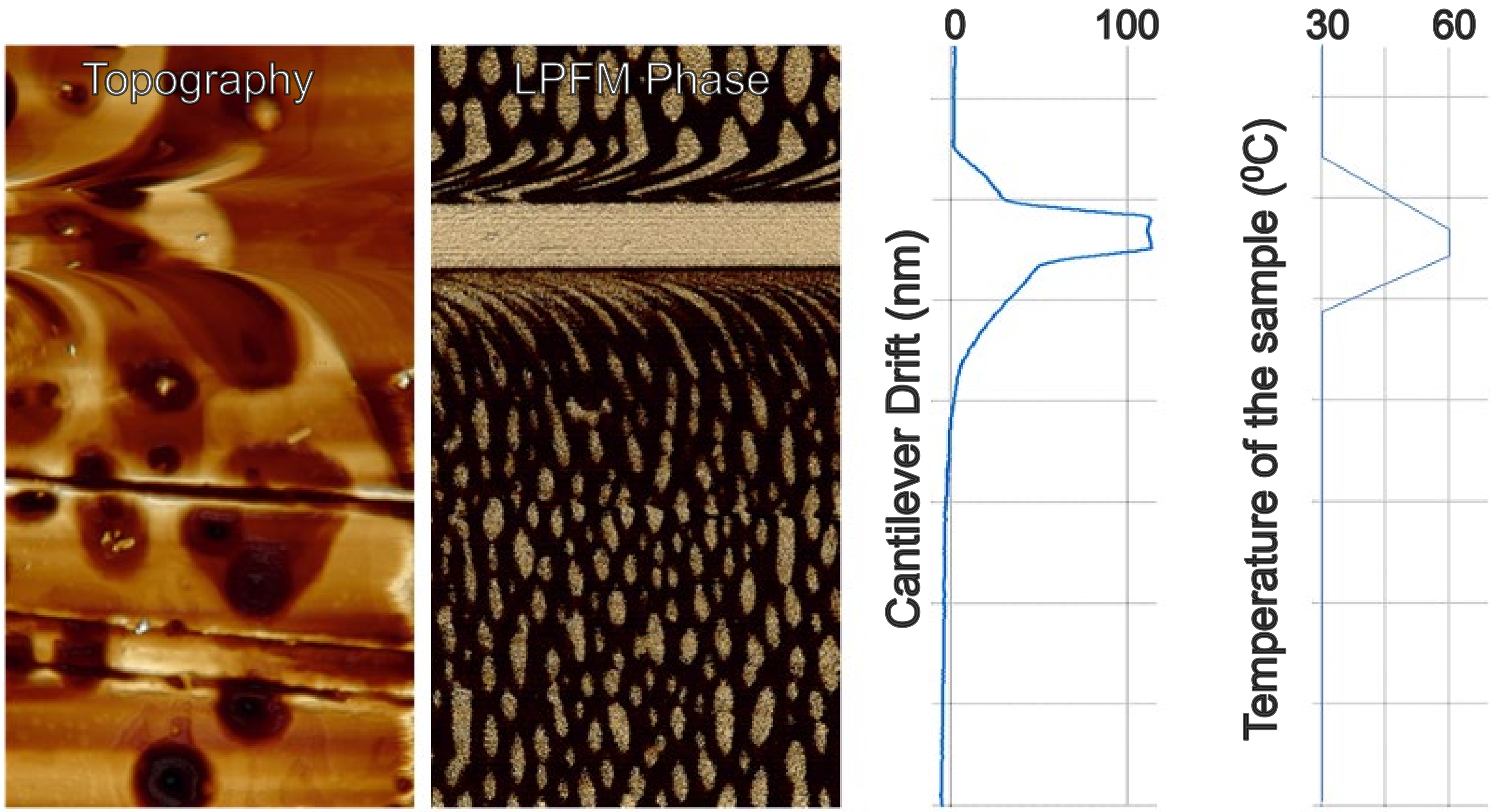

In-situ HD PFM study of second-order phase transition of triglycine sulfate crystal. Scan size 15×15 µm. Sample courtesy: Dr. R. Gainutdinov, IC RAS

Kelvin Probe Microscopy

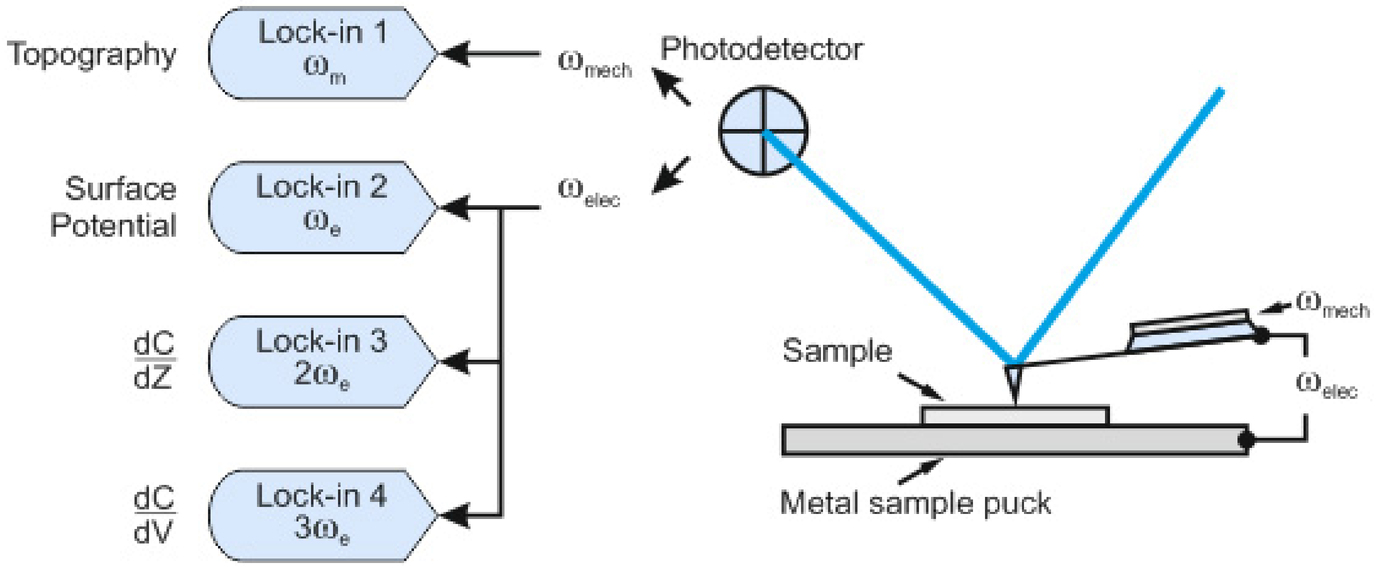

Electrostatic interaction between probe and sample

$$F_z = F_{z,DC} + F_{z,\omega} + F_{z,2\omega}$$

$$F_{z,DC} = -\left[\frac{1}{2}\times\left((U_0-\varphi(x,y))^2+\frac{1}{2}\times U_1^2\right)\right]\times\frac{\partial C}{\partial Z}$$

$$F_{z,\omega} = -\left[(U_0-\varphi(x,y))\times U_1\times\sin(\omega t)\right]\times\frac{\partial C}{\partial Z}$$

$$F_{z,2\omega} = \left[\frac{1}{4}\times U_1^2\times\cos(2\omega t)\right]\times\frac{\partial C}{\partial Z}$$

KPFM studies of graphene at variable RH

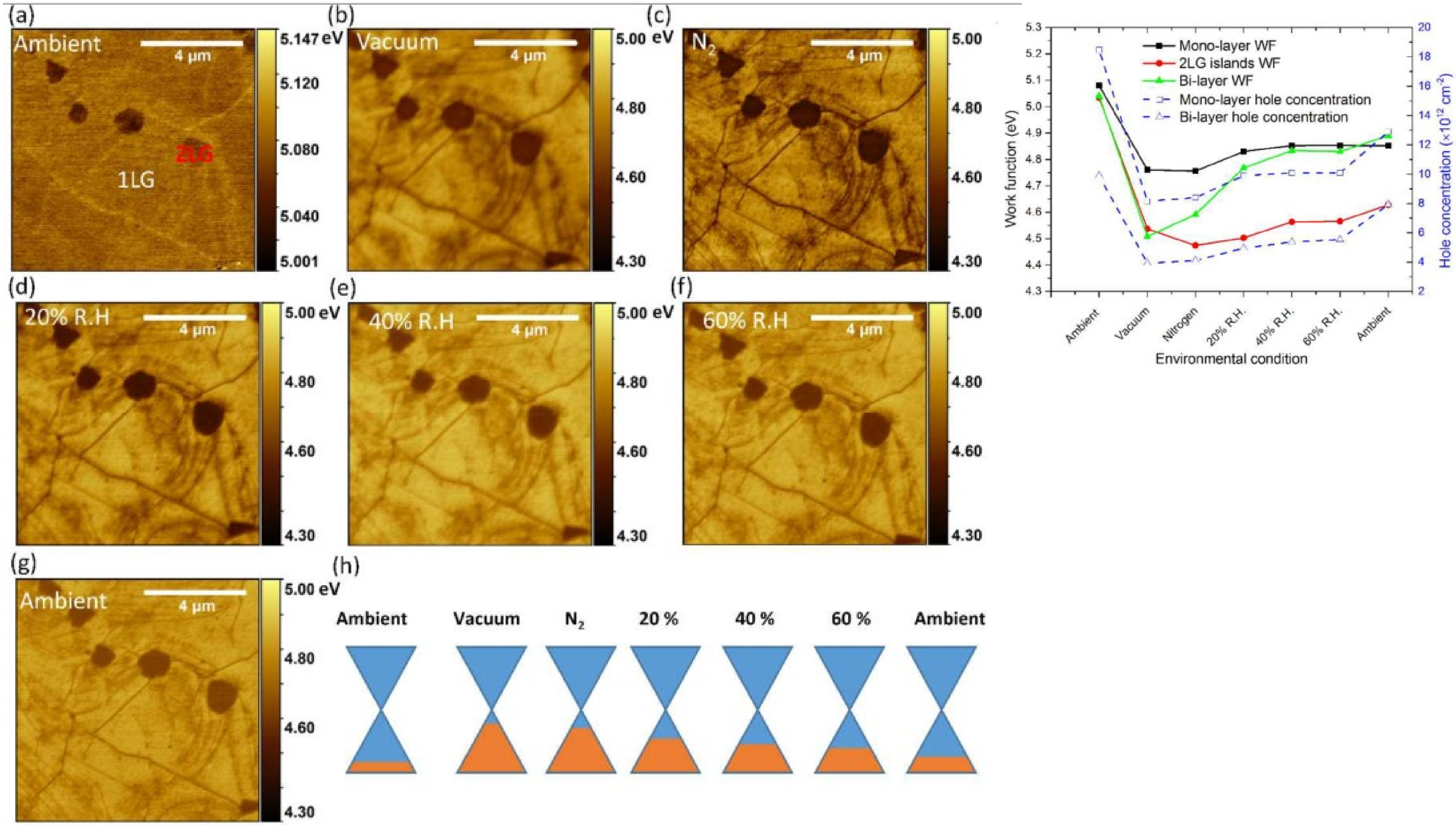

C. Melios, A. Centeno, A. Zurutuza, V. Panchal, C. Giusca, S. Spencer, S. Silva and O. Kazakova, "Effects of humidity on the electronic properties of graphene prepared by chemical vapour deposition", *Carbon*, vol. 103, pp. 273-280, 2016.

NT-MDT Spectrum Instruments

Magnetic Force Microscopy (MFM)

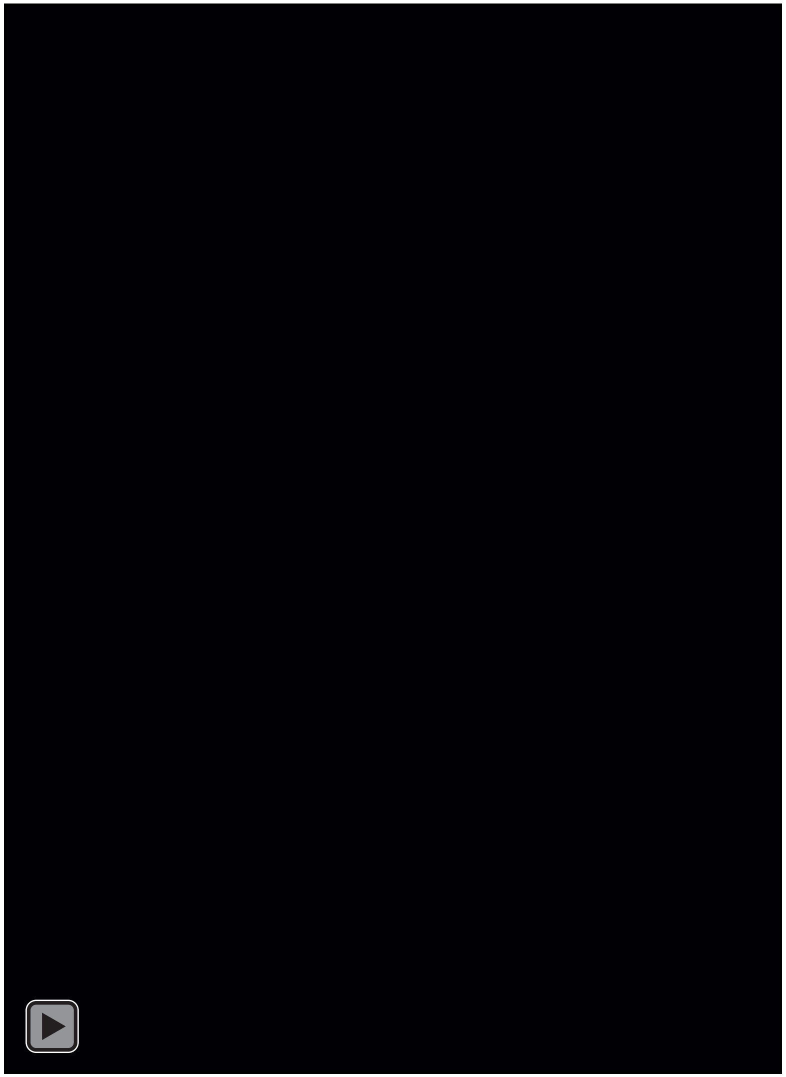

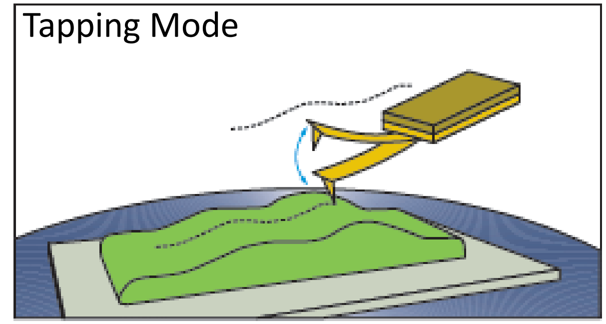

MFM Studies of Co/Pt Nanowires

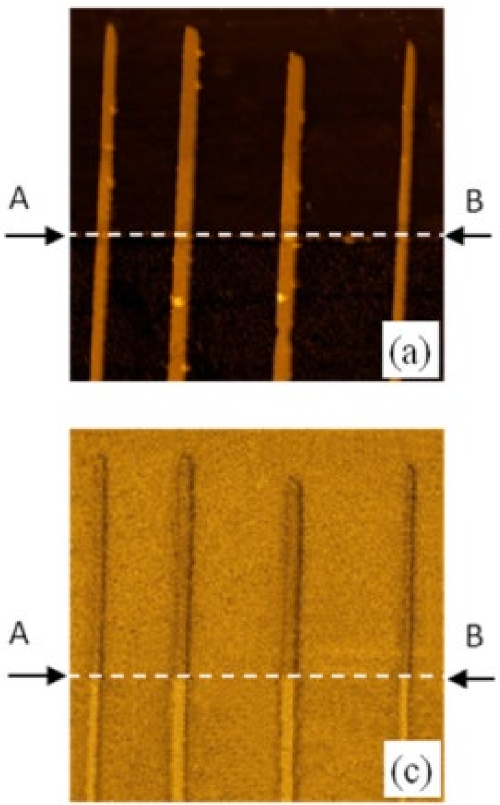

NTEGRA AFM Setup with in-plane external magnet

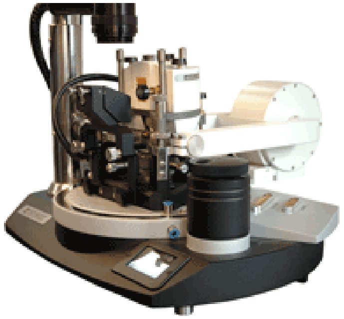

The sequential stages of remagnetization for Co/Pt NWs partly covered by Co capping layer.
(a) The AFM image of the sample with Co/Pt NWs. The area below line A-B is covered by Co (1.3 nm) The frame sizes are 1.5 µm × 1.5 µm. The MFM contrast is normalized to the maximum. The border of Co capping layer is shown by arrows and dashed line; (b) The MFMimage of up-magnetized sample; (c) The MFM image of partly remagnetized NWs after applying of 150 Oe reversed magnetic field; (d) The MFM image of down-magnetized NWs in the field of 200 Oe. The frame sizes are 1.5 µm × 1.5 µm. The MFM contrast is normalized to the maximum.

O. Ermolaeva, N. Gusev, E. Skorohodov, Y. Petrov, M. Sapozhnikov and V. Mironov, "Magnetic Force Microscopy of Nanostructured Co/Pt Multilayer Films with Perpendicular Magnetization", *Materials*, vol. 10, no. 9, p. 1034, 2017.

NT-MDT Spectrum Instruments

Nanolithography (Electrical Way)

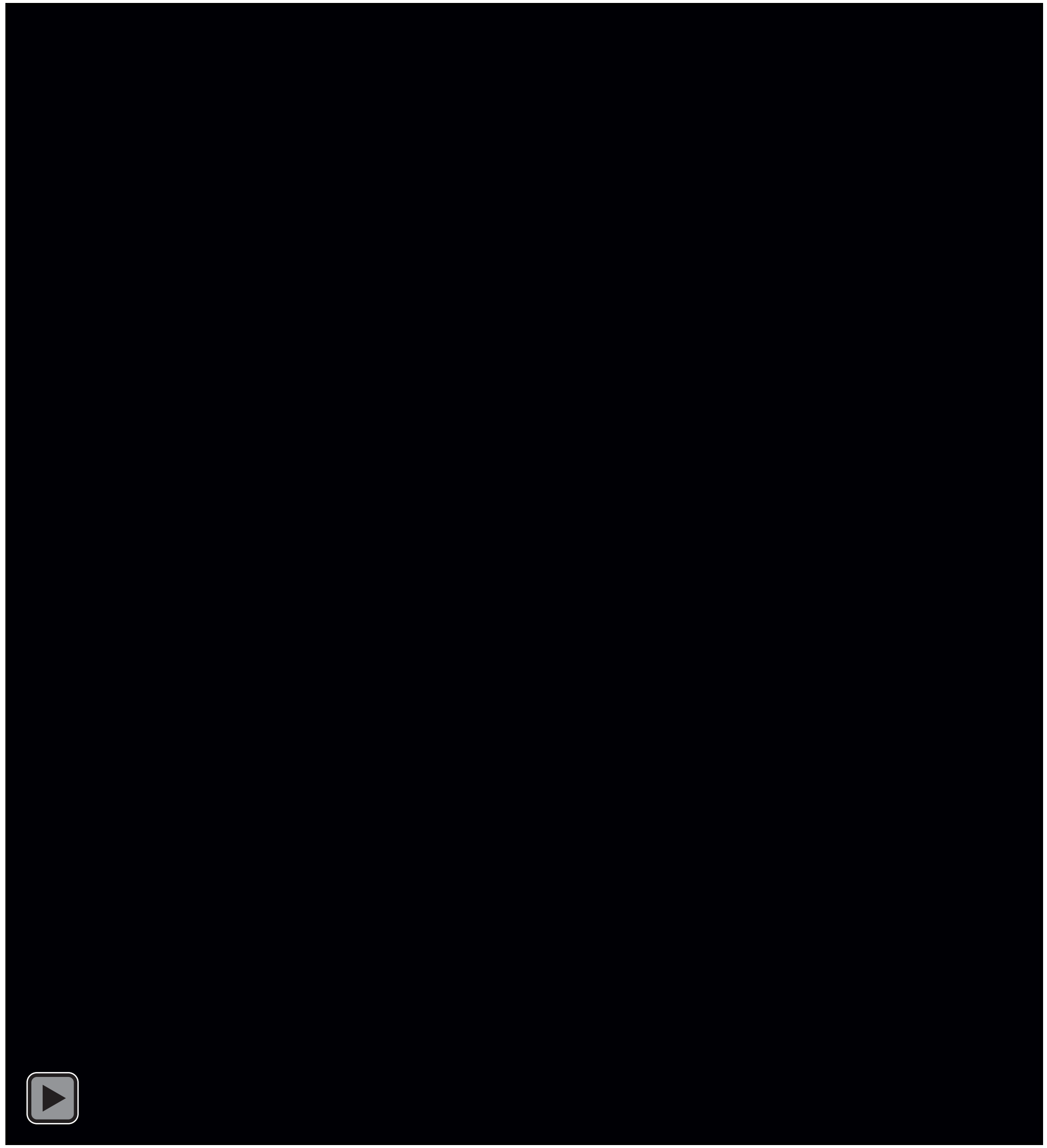

Nanopatterning on carboxyl-terminated silane monolayers

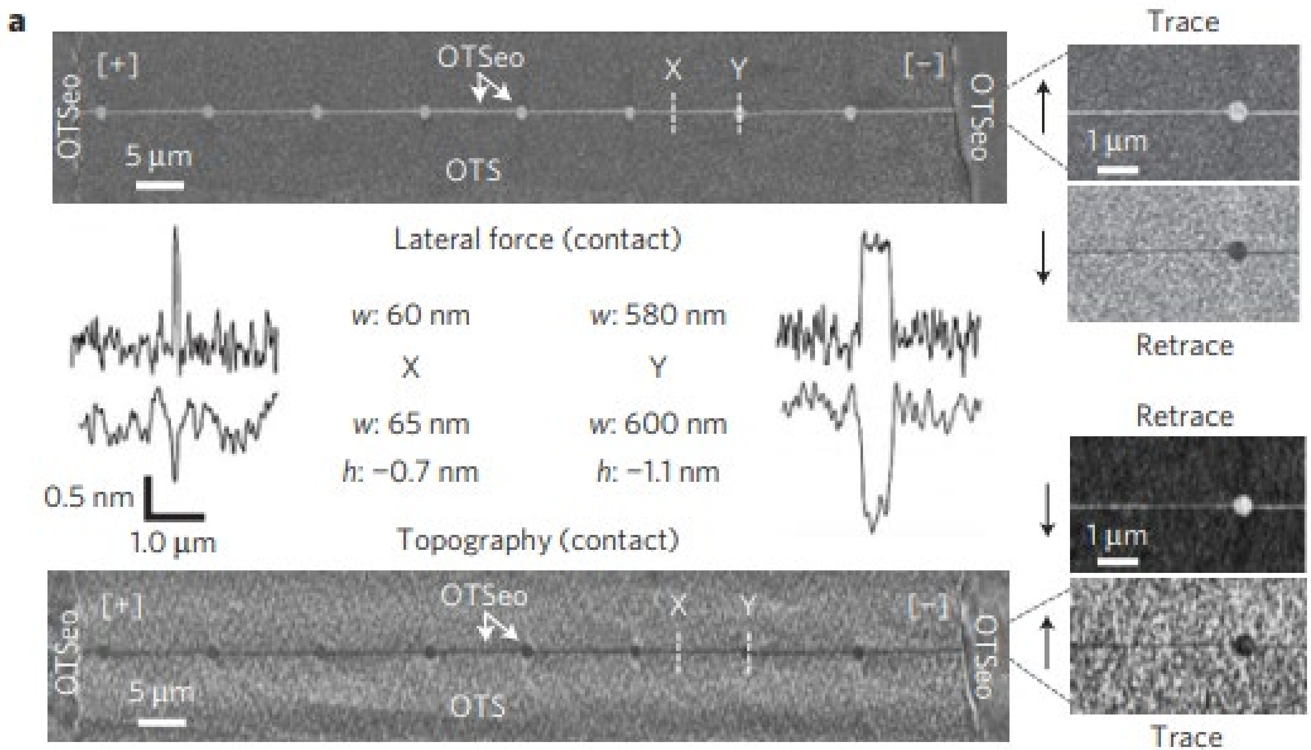

Experimental results obtained with the ion-conducting macro–micro–nano-channel.

AFM images of the OTSeo@OTS nano–micro-channel constriction connecting two large OTSeo@OTS macro-channels with a total area of 2.27 cm^2 taken after the acquisition of all electrical data from this specimen.

J. Berson, D. Burshtain, A. Zeira, A. Yoffe, R. Maoz and J. Sagiv, "Single-layer ionic conduction on carboxyl-terminated silane monolayers patterned by constructive lithography", *Nature Materials*, vol. 14, no. 6, pp. 613-621, 2015.

NT-MDT Spectrum Instruments

Reversible Nanopatterning of Polypyrrole Films

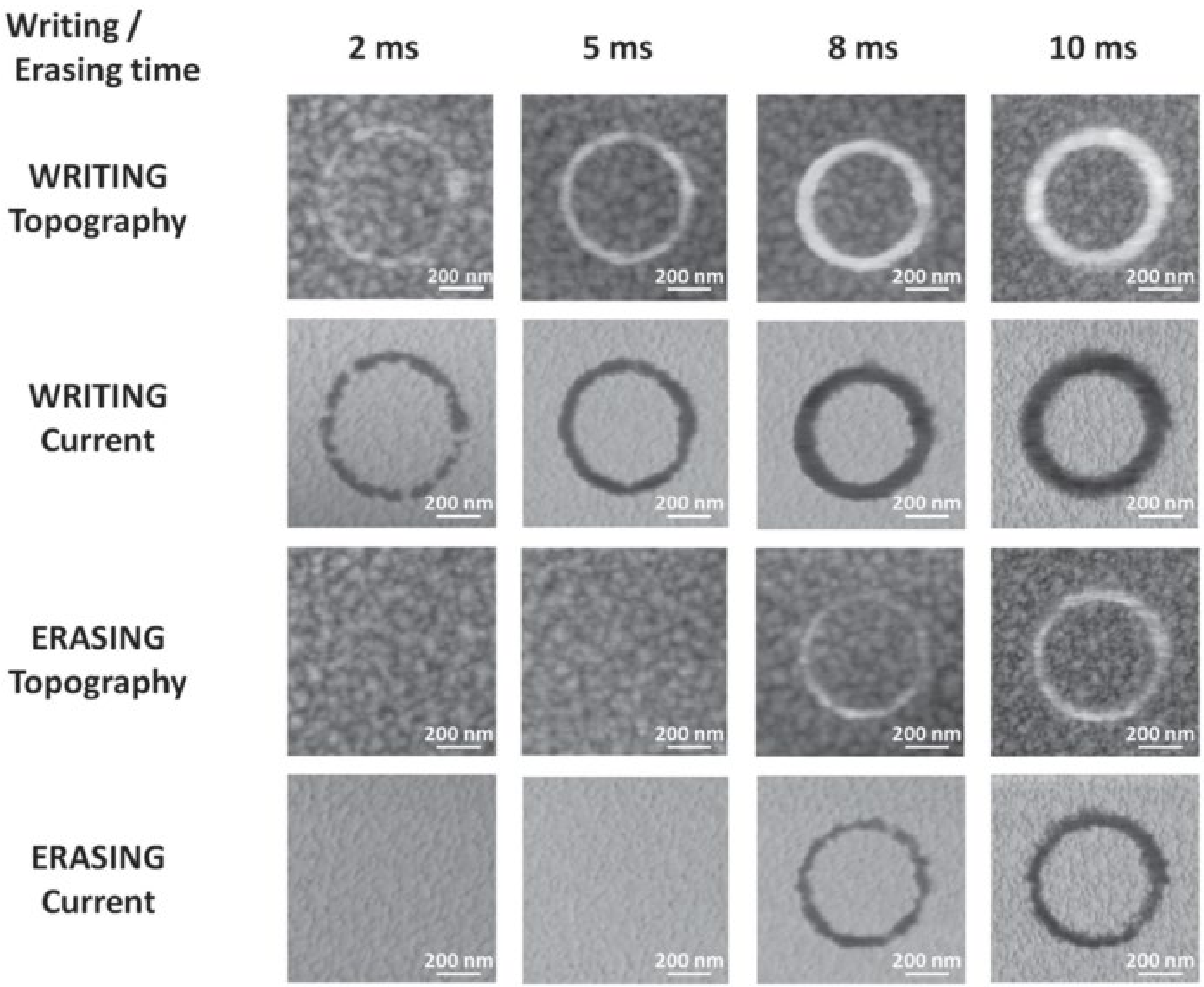

Comparison of the writing and erasing processes using different operation times. The size of each image is 1 µm × 1 µm. potentiostatically

H. Liu, S. Hoeppener and U. Schubert, "Reversible Nanopatterning on Polypyrrole Films by Atomic Force Microscope Electrochemical Lithography", *Advanced Functional Materials*, vol. 26, no. 4, pp. 614-619, 2015.

NT-MDT
Spectrum Instruments

Combination with Optical Techniques

Combination with Optical Techniques

NTEGRA SPECTRA

1998-2018

20 years of expertise

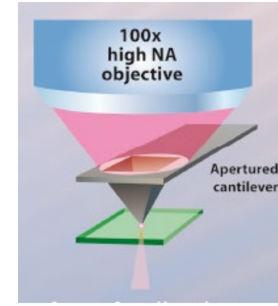

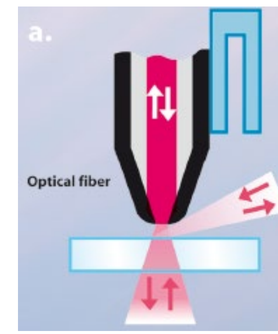

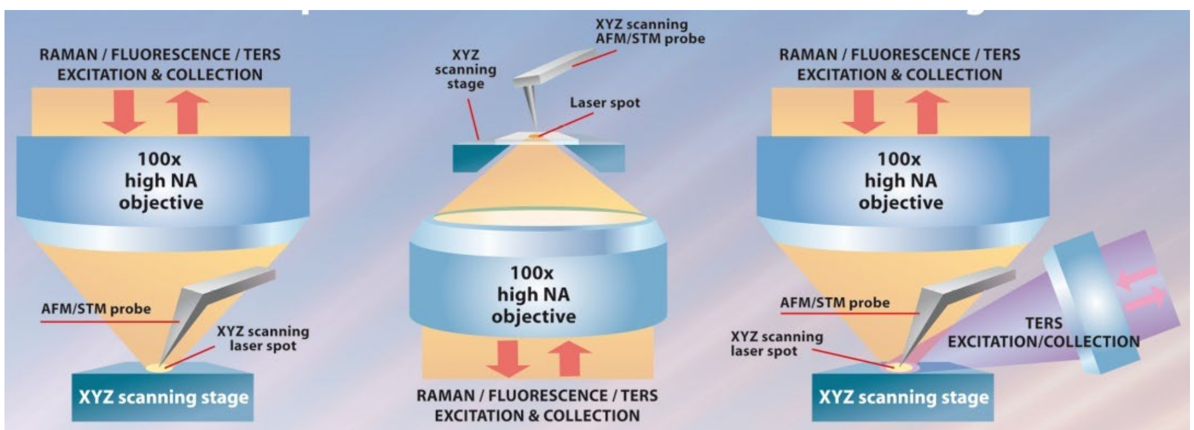

NTEGRA SPECTRA II

Power of AFM-Raman Combination

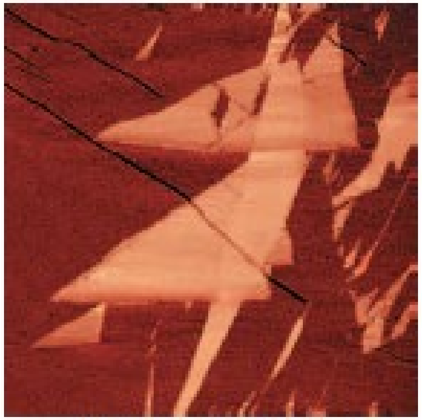

AFM: Force modulation (elastic properties)

AFM: Electrostatic force (charge distribution)

AFM: Kelvin probe microscopy (surface potential)

AFM: Lateral force (friction)

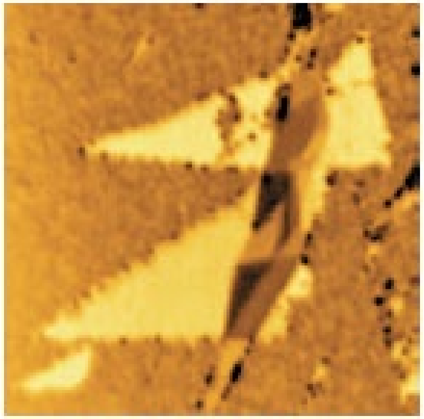

Rayleigh light intensity (473 nm laser)

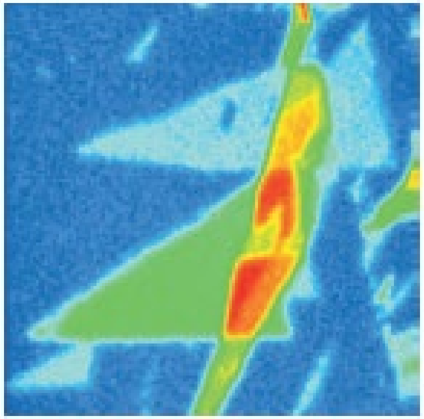

Confocal Raman map: G-band intensity

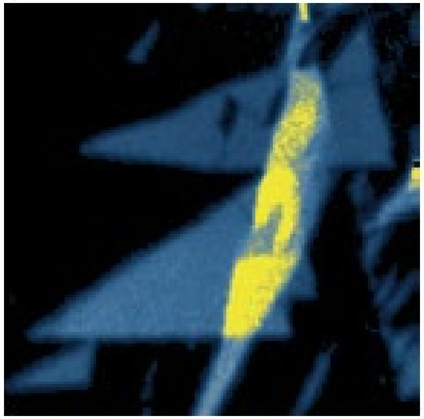

Confocal Raman map: 2D (G') band mass center

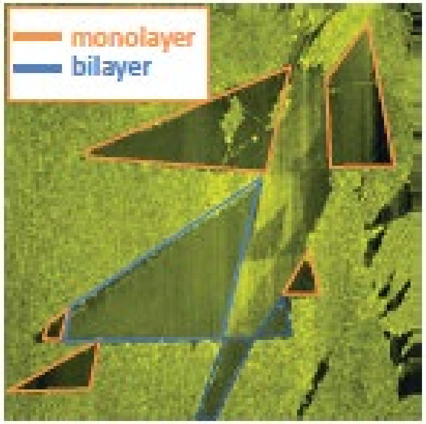

AFM: Height (topography) Size: 30×30 µm. Substrate: gold

TERS: Tip Enhanced Raman Scattering

Raman/Fluorescence microscopy with subwavelength spatial resolution

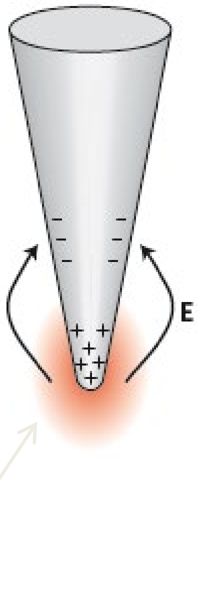

Localized surface plasmon at the end of nanoantenna

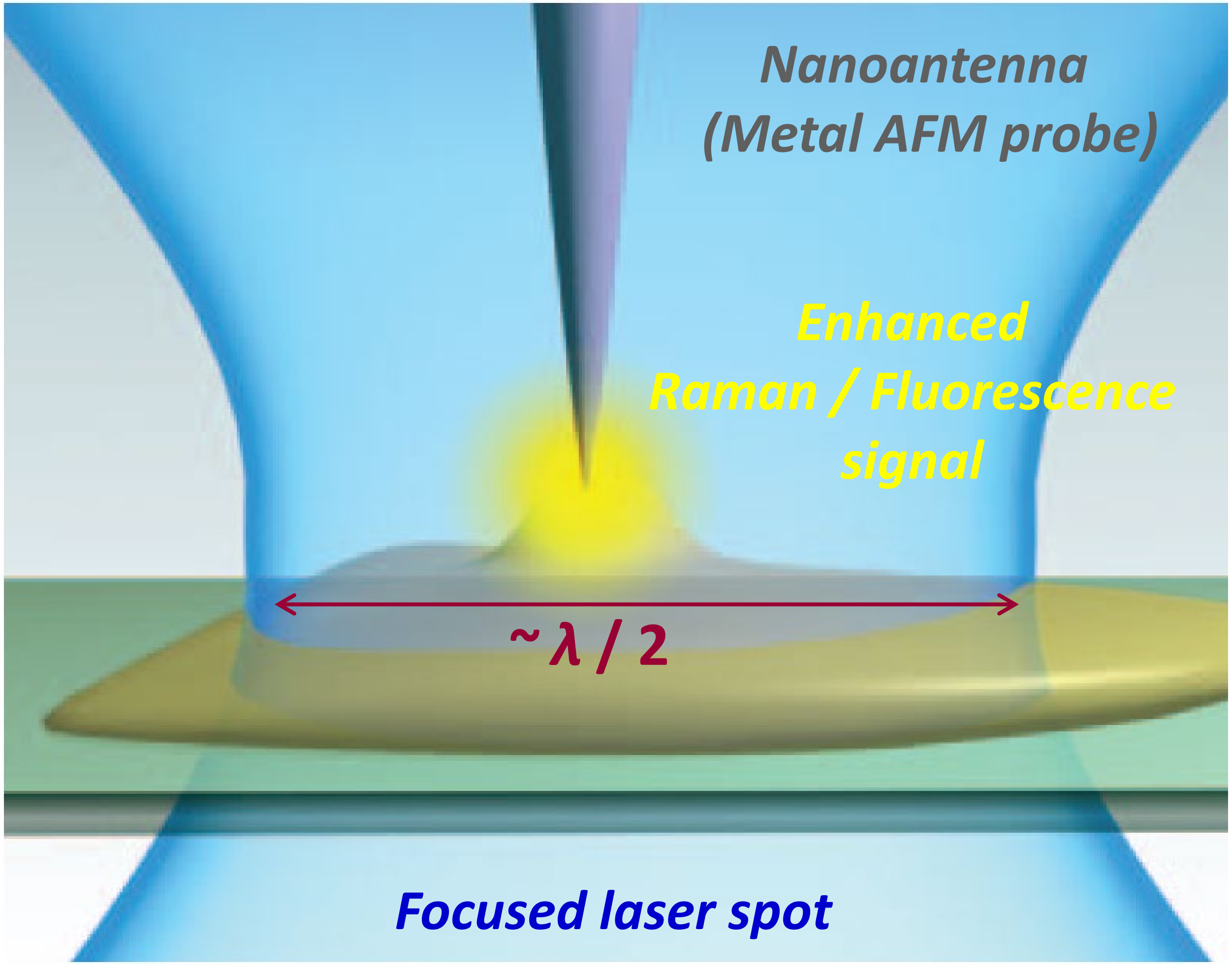

Graphene structure visualized by TERS

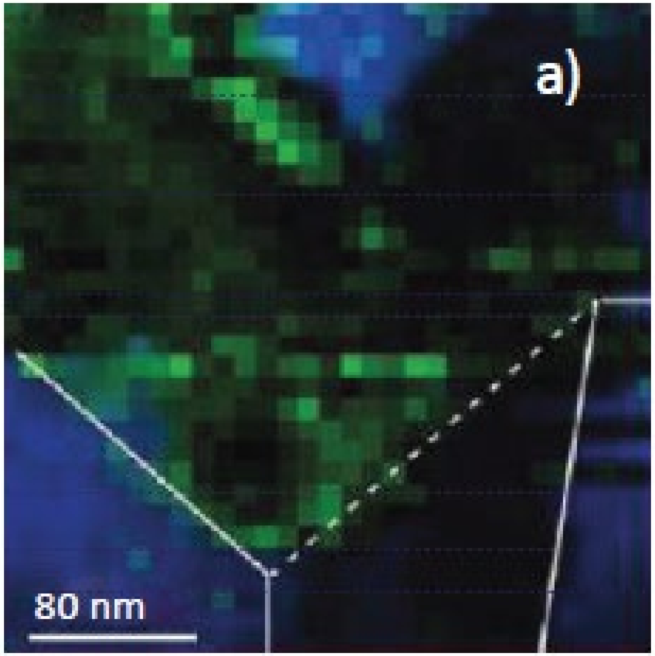

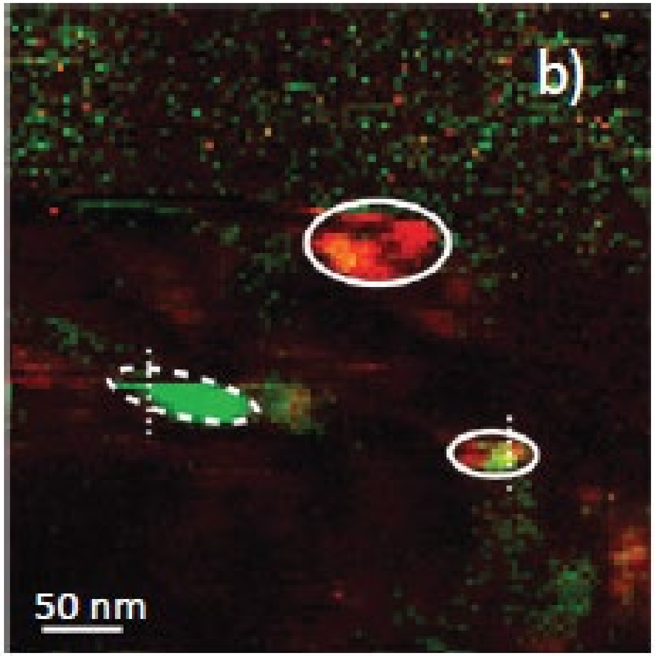

(a) TERS maps of single layer CVD Graphene on copper substrate. Green color: areas of pristine graphene (2D band intensity). Blue color: CH-terminated graphene areas (CHbands intensity). (b) TERS map of mechanically exfoliated single layer graphene on Au substrate. Green color: 2D band intensity. Red color: Dband intensity (areas with strong defects). Resolution of all Raman maps is <12 nm.

J. Stadler, T. Schmid, and R. Zenobi, Nano Letters (2010) , 10, 4514-4520 .

NT-MDT Spectrum Instruments

NTEGRA Nano IR: IR s-SNOM measurements

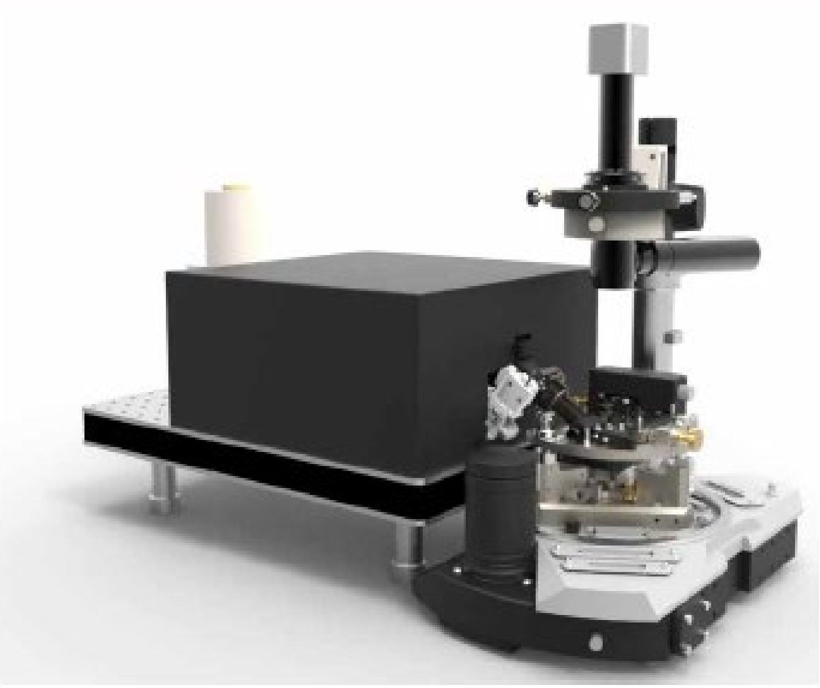

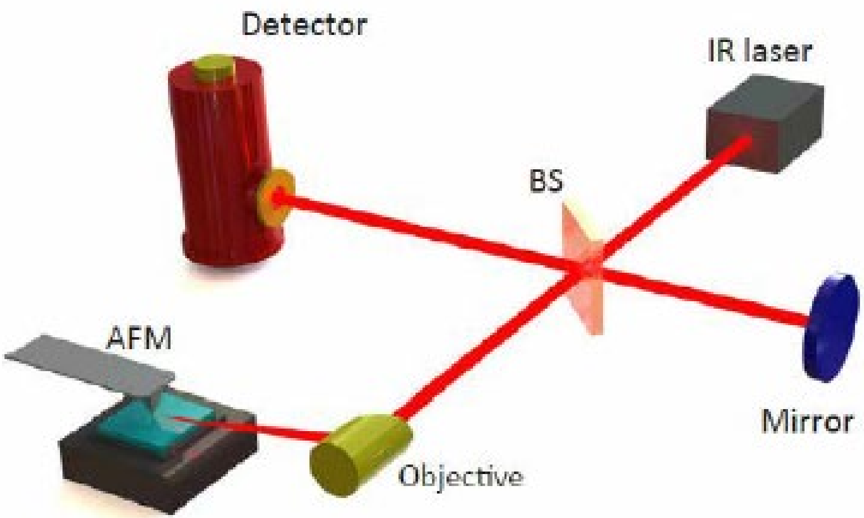

NTEGRA IR principal scheme

- IR s-SNOM microscopy and spectroscopy with 10 nm spatial resolution
- Wide spectral range of operation: 3-12 µm
- Incredibly low thermal drift and high signal stability
- Versatile AFM with advanced modes: SRI (conductivity), KPFM (surface potential), SCM (capacitance), MFM (magnetic properties), PFM (piezoelectric forces)
- HybriD Mode™ - quantitative nanomechanical mapping
- Integration with microRaman (optional)

NT-MDT Spectrum Instruments

High Temperature AFM and s-SNOM on a Phase Changing Material: VO_2

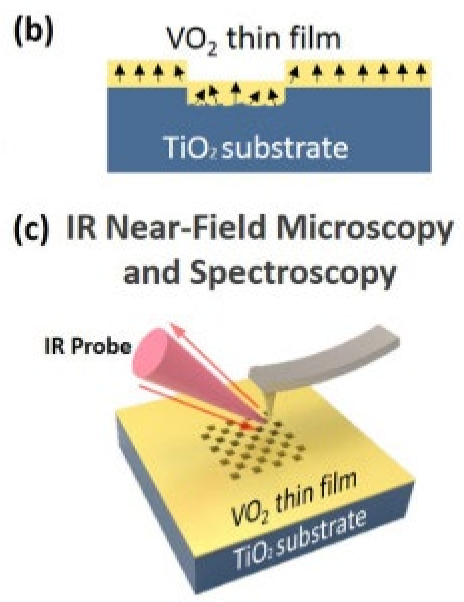

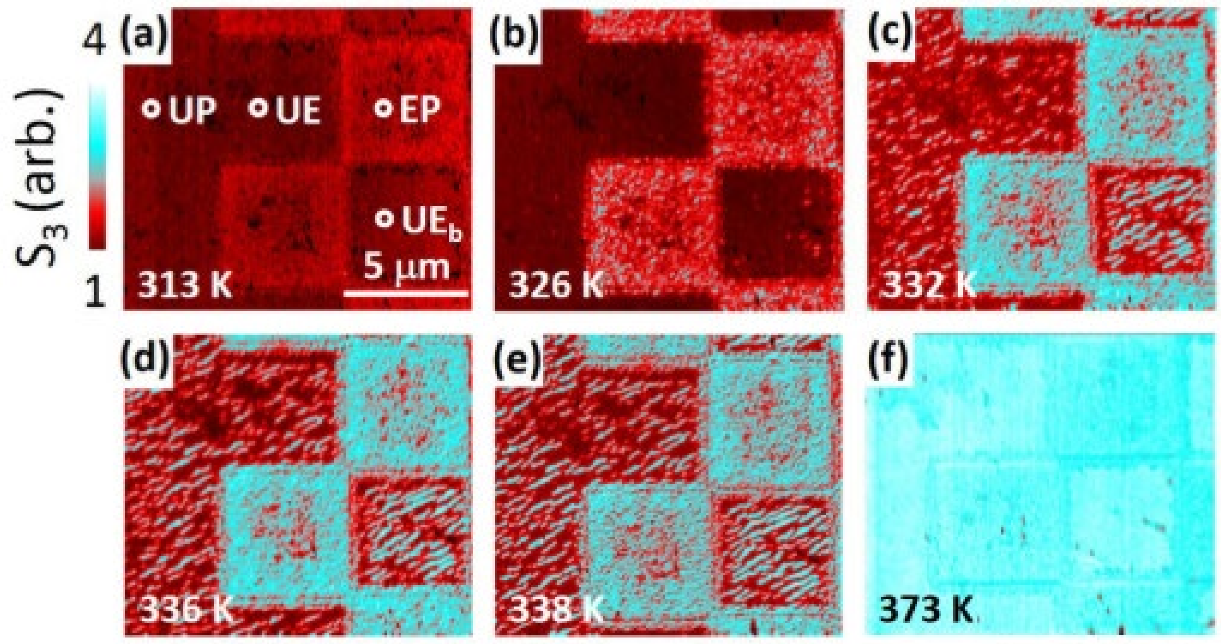

Temperature-dependent infrared near-field images of patterned VO2/TiO2 at 11 μm, revealing area-dependent insulator-to- metal phase transitions. The metallic phase is shown in cyan and the insulating phase in red

Gilbert Corder, S. et al. Controlling phase separation in vanadium dioxide thin films via substrate engineering. *Physical Review B* 96, (2017).

NT-MDT Spectrum Instruments

High Temperature AFM and s-SNOM on a Phase Changing Material: VO_2

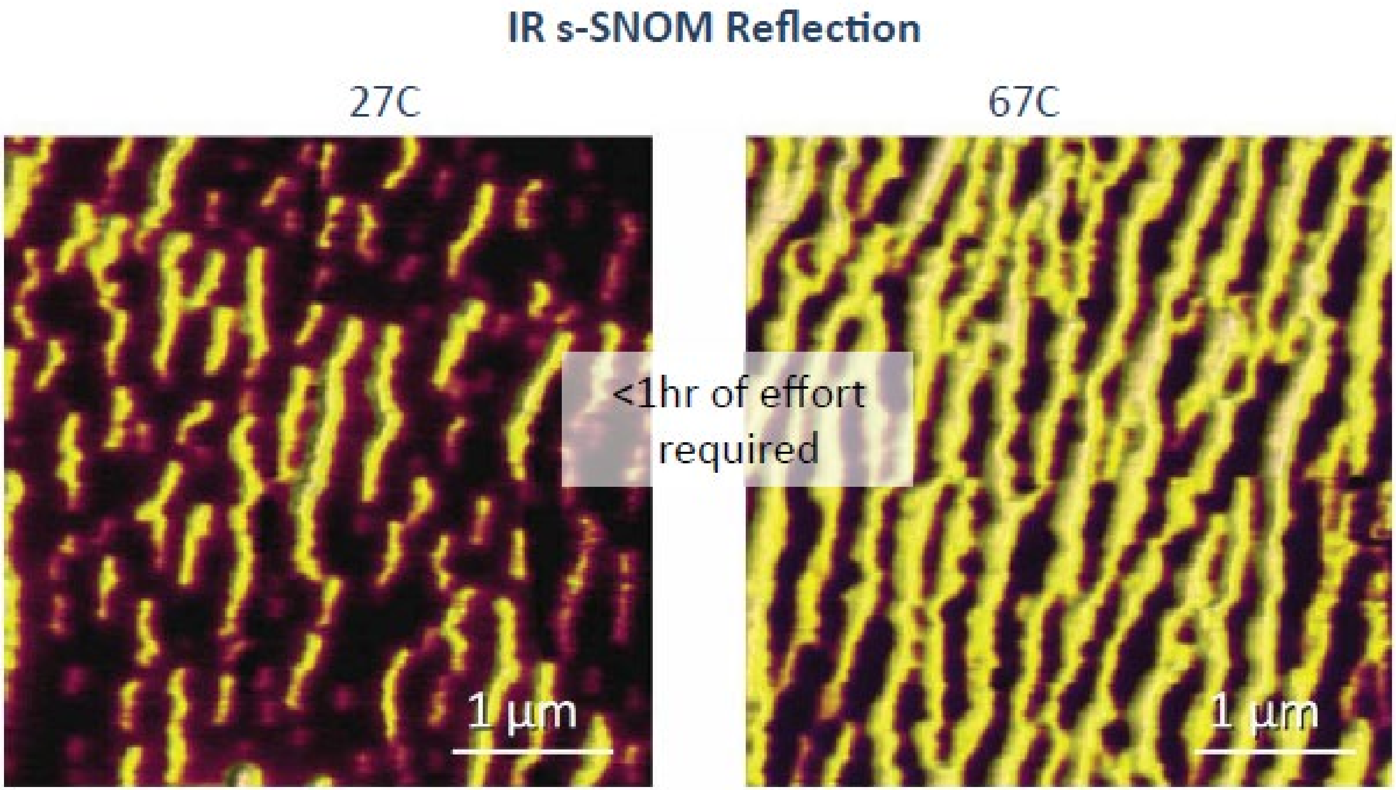

- Superior high temperature performance: under 1 hour needed to acquire images 40C apart. Compare to days on competitor's system
- Low drift and high signal stability: <1um XY drift from 27 to 67C, no realignment of nanoReflection optics needed

Sample courtesy to prof. Liu (Stony Brook University, New York, USA)

NT-MDT Spectrum Instruments

IR s-SNOM: Ultrathin film of oligothiophene monolayers on silicon

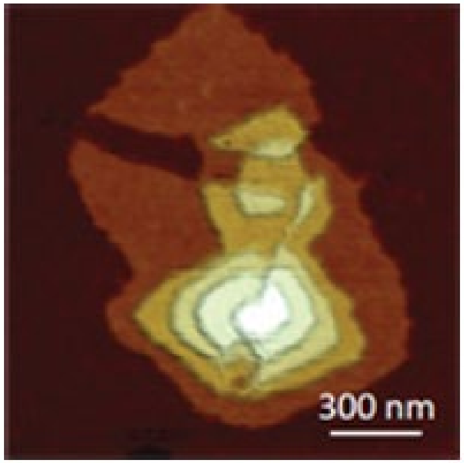

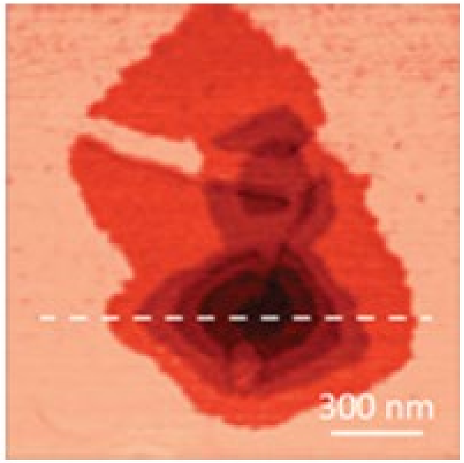

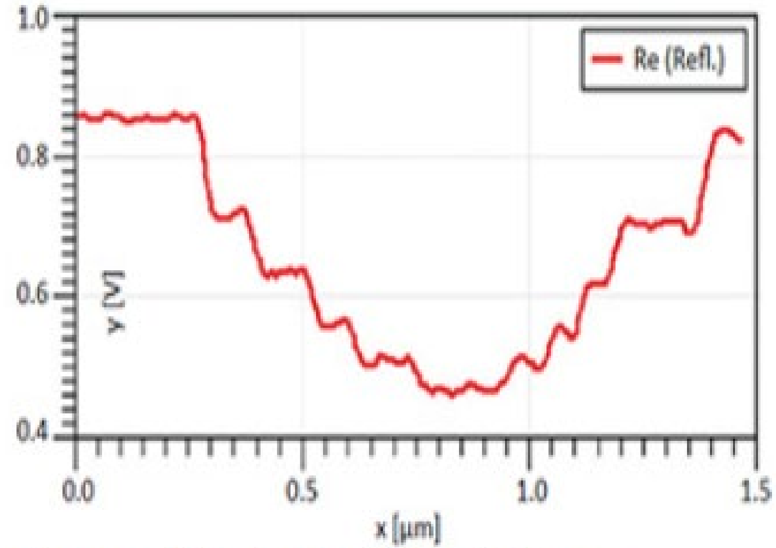

IR reflection contrast of thin and soft structures easily detectable. Each of five 3.4 nm steps is resolved. Spatial resolution is better than λ/1000.

Sample courtesy to Dr. A. Mourran (DWI, Aachen, Germany). Measured by Dr. G. Andreev (EVS Co)

NT-MDT Spectrum Instruments Product Line

AFM

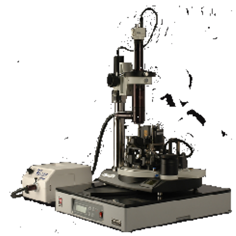

SOLVER NANO

- Compact desktop AFM/STM for both education and science
- Full set of AFM/STM modes
- High AFM/STM performance
- Closed-loop Scanner

NEXT/ TITANIUM

- AFM/STM with exceptional level of automation
- Fast, precise and low-noise closed-loop scanner
- High resolution imaging due to extremely low noise and high stability
- Full set of standard and advanced AFM/STM modes
- HybriD Mode™

NTEGRA

- Modular high performance AFM/STM for wide range of applications
- Low noise and high resolution
- Full set of standard and advanced AFM/STM modes
- HybriD Mode™

VEGA

- Automated high-resolution AFM for up to 200x200 mm samples
- Ultra stable AFM
- Full set of standard and advanced AFM modes
- HybriD Mode™
- ScanTronic™

AFM-Raman / IR / TERS

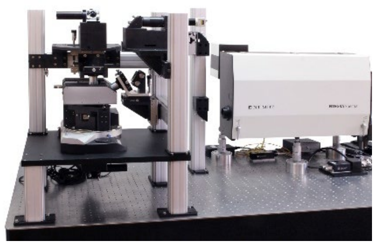

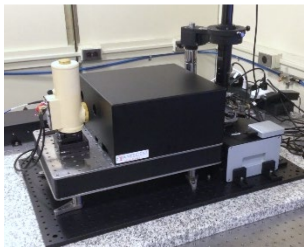

NTEGRA SPECTRA II

- SPM
- Automated AFM laser, probe and photodiode
- Confocal Raman / Fluorescence / Rayleigh Microscopy
- Tip Enhanced Raman Scattering (TERS)
- TERS optimized system for all possible excitation/detection geometries
- HybriD Mode™

NTEGRA Nano IR

- IR sSNOM system
- High resolution AFM
- Stabilized CO_2 laser
- HybriD Mode™

References

- D. Bagrov, Y. Gazizova, V. Podgorsky, I. Udovichenko, A. Danilkovich, K. Prusakov and D. Klinov, "Morphology and aggregation of RADA-16-I peptide Studied by AFM, NMR and molecular dynamics simulations", *Biopolymers*, vol. 106, no. 1, pp. 72-81, 2016.
- Eidelshtein, G., Fardian-Melamed, N., Gutkin, V., Basmanov, D., Klinov, D., Rotem, D., Levi-Kalisman, Y., Porath, D. & Kotlyar, A. DNA-Metalization: Synthesis and Properties of Novel Silver-Containing DNA Molecules (Adv. Mater. 24/2016). *Advanced Materials* 28, 4944-4944 (2016).
- Jelken, J., Pandiyarajan, C., Genzer, J., Lomadze, N. & Santer, S. Fabrication of Flexible Hydrogel Sheets Featuring Periodically Spaced Circular Holes with Continuously Adjustable Size in Real Time. *ACS Applied Materials & Interfaces* 10, 30844-30851 (2018).
- H. Schniepp, S. Koebley and F. Vollrath, "Brown Recluse Spider's Nanometer Scale Ribbons of Stiff Extensible Silk", *Advanced Materials*, vol. 25, no. 48, pp. 7028-7032, 2013.
- Wang, Q. & Schniepp, H. Strength of Recluse Spider’s Silk Originates from Nanofibrils. *ACS Macro Letters* 7, 1364-1370 (2018).
- S. Magonov, S. Belikov, J. D. Alexander, C. G. Wall, S. Leesment, and V. Bykov, “Scanning probe based apparatus and methods for low-force profiling of sample surfaces and detection and mapping of local mechanical and electromagnetic properties in non-resonant oscillatory mode,” US9110092B1.
- M. Xu, B. Liu, G. Graham and X. Pan, "High resolution characterization of grain boundaries in Cu 2 ZnSnSe4 solar cells synthesized by nanoparticle selenization", *Solar Energy Materials and Solar Cells*, vol. 157, pp. 171-177, 2016.
- J. Montenegro, C. Vázquez-Vázquez, A. Kalinin, K.E. Geckeler, J.R. Granja, Coupling of carbon and peptide nanotubes, *J. Am. Chem. Soc.* 136 (2014) 2484–2491

References

- B. Stojadinović, B. Vasić, D. Stepanenko, N. Tadić, R. Gajić and Z. Dohčević-Mitrović, "Variation of electric properties across the grain boundaries in BiFeO3film", *Journal of Physics D: Applied Physics*, vol. 49, no. 4, p. 045309, 2015.
- Kholkin, A., Amdursky, N., Bdikin, I., Gazit, E., & Rosenman, G. (2010) ACS nano, 4(2), 610-614.
- Ivanov, M., Kopyl, S., Tofail, S. A., Ryan, K., Rodriguez, B. J., Shur, V. Y., & Kholkin, A. L. (2016) In Electrically Active Materials for Medical Devices (pp. 149-166).
- A. Kalinin, V. Atepalikhin, O. Pakhomov, A. Kholkin and A. Tselev, "An atomic force microscopy mode for nondestructive electromechanical studies and its application to diphenylalanine peptide nanotubes", *Ultramicroscopy*, vol. 185, pp. 49-54, 2018.
- M. Konečný et al. "Kelvin Probe Force Microscopy and Calculation of Charge Transport in a Graphene/Silicon Dioxide System at Different Relative Humidity", *ACS Applied Materials & Interfaces*, vol. 10, no. 14, pp. 11987-11994, 2018.
- O. Ermolaeva, N. Gusev, E. Skorohodov, Y. Petrov, M. Sapozhnikov and V. Mironov, "Magnetic Force Microscopy of Nanostructured Co/Pt Multilayer Films with Perpendicular Magnetization", *Materials*, vol. 10, no. 9, p. 1034, 2017.
- J. Berson, D. Burshtain, A. Zeira, A. Yoffe, R. Maoz and J. Sagiv, "Single-layer ionic conduction on carboxyl-terminated silane monolayers patterned by constructive lithography", *Nature Materials*, vol. 14, no. 6, pp. 613-621, 2015.
- H. Liu, S. Hoeppener and U. Schubert, "Reversible Nanopatterning on Polypyrrole Films by Atomic Force Microscope Electrochemical Lithography", *Advanced Functional Materials*, vol. 26, no. 4, pp. 614-619, 2015.
- *J. Stadler, T. Schmid, and R. Zenobi, Nano Letters (2010) , 10, 4514-4520*
- *Gilbert Corder, S. et al.* Controlling phase separation in vanadium dioxide thin films via substrate engineering. *Physical Review B* 96, (2017).

NT-MDT
Spectrum Instruments

Acknowledgements

Dr. V. Bykov
Dr. V. Polyakov
Dr. Y. Bobrov
Dr. A. Kalinin
Dr. A. Shelaev
Dr. S. Magonov
Dr. P. Dorozhkin
S. Nesterov

Thank you for your attention!

Q&A

NT-MDT
Spectrum Instruments

www.ntmdt-si.com